

RESEARCH ARTICLE SUMMARY

NEUROSCIENCE

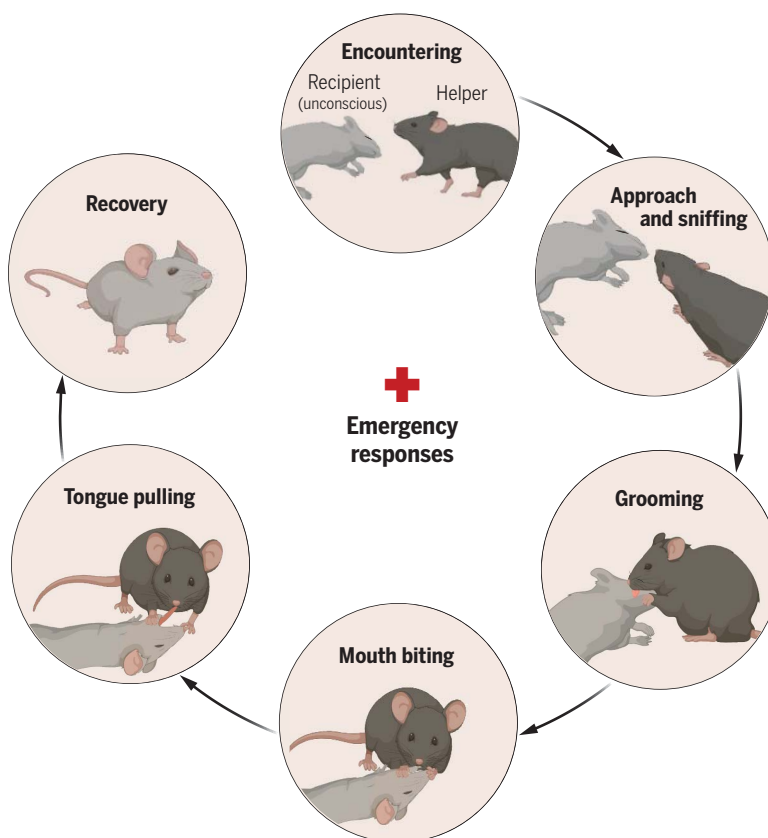
Reviving-like prosocial behavior in response to unconscious or dead conspecifics in rodents

Wenjian Sun[†], Guang-Wei Zhang[†], Junxiang J. Huang, Can Tao, Michelle B. Seo, Huizhong Whit Tao*, Li I. Zhang*

INTRODUCTION: When humans encounter someone unconscious, they often respond with emergency reactions aimed at reviving that person. However, it remains unclear whether animals naturally exhibit any specific behaviors when faced with an unconscious peer.

RATIONALE: Anecdotal observations of various animal species in the wild have documented behaviors toward peers that have collapsed as a result of sickness, injury, or death. These behaviors include touching, grooming, nudging, and sometimes even more intense physical ac-

tions such as striking. Although these actions toward incapacitated conspecifics are reminiscent of human emergency responses involving intense sensory stimulation, it remains difficult to determine the precise nature of these behaviors, how common they are within a species, and the neural mechanisms behind them. In this study, using laboratory mice under controlled conditions, we examined whether animals naturally display any stereotypic behaviors in response to and directed toward their unresponsive social partners, which would allow us to address the above questions.



Mouse behaviors toward an unconscious peer. Mice exhibit a stereotypic set of behaviors when encountering an unconscious social partner, reminiscent of human emergency responses. The behavioral reactions escalate from sniffing and grooming to intense stimulatory actions such as mouth biting and tongue pulling during extended periods of unresponsiveness. These reviving-like actions facilitate the recipient's recovery. [Figure created with BioRender.com]

RESULTS: Behavioral monitoring combined with a machine learning-based annotator showed that when mice encountered a familiar social partner in a state of unconsciousness caused by anesthesia, they displayed distinct and consistent behaviors toward the partner, escalating from sniffing and grooming to more forceful actions such as biting the partner's mouth or tongue and pulling its tongue out. The latter intense actions were also observed in mice interacting with a dead familiar partner but were rarely seen when the partner was active or simply sleeping. These behaviors emerged after prolonged immobility and unresponsiveness of the partner and ceased once the partner regained activity, suggesting that they were triggered by observing unresponsive states of others. These behaviors were strongly influenced by familiarity, being more pronounced in familiar pairs, and were unlikely to have been motivated by a desire for reciprocal social interaction or curiosity about something new. The consequences—including clearance of foreign objects from the mouth, improved airway opening, and hastened recovery—suggest reviving-like efforts. Electrophysiological recordings and microendoscopic calcium imaging showed that oxytocin neurons in the hypothalamic paraventricular nucleus as a population exhibited increased activation in the presence of unconscious, compared with active, familiar partners, suggesting that the activity of these neurons can distinguish between the different partner states. Additionally, increased activity was observed in distinct subpopulations of the oxytocin neurons during specific behavioral actions. Furthermore, optogenetic activation of these neurons promoted reviving-like behaviors, whereas inactivation of them or blocking oxytocin signaling through ventricular administration of oxytocin receptor antagonists impaired the behaviors.

CONCLUSION: Our study reveals a stereotypic set of behaviors in mice directed toward unresponsive familiar peers that appear to facilitate the regaining of responsiveness. Similar to other prosocial behaviors, these behaviors rely on the oxytocin system, which is essentially conserved across vertebrate species. Our findings thus suggest that animals exhibit reviving-like emergency responses and that assisting unresponsive group members may be an innate behavior widely present among social animals. Such behavior likely plays a role in enhancing group cohesion and survival. ■

The list of author affiliations is available in the full article online.

*Corresponding author. Email: liizhang@usc.edu (L.I.Z.); htao@usc.edu (H.W.T.)

†These authors contributed equally to this work.
Cite this article as W. Sun et al., *Science* **387**, eadq2677 (2025). DOI: 10.1126/science.adq2677

S READ THE FULL ARTICLE AT
<https://doi.org/10.1126/science.adq2677>

RESEARCH ARTICLE

NEUROSCIENCE

Reviving-like prosocial behavior in response to unconscious or dead conspecifics in rodents

Wenjian Sun^{1†}, Guang-Wei Zhang^{1†}, Junxiang J. Huang^{1,2}, Can Tao¹, Michelle B. Seo^{1,3}, Huizhong Whit Tao^{1,4*}, Li I. Zhang^{1,4*}

Whereas humans exhibit emergency responses to assist unconscious individuals, how nonhuman animals react to unresponsive conspecifics is less well understood. We report that mice exhibit stereotypic behaviors toward unconscious or dead social partners, which escalate from sniffing and grooming to more forceful actions such as mouth or tongue biting and tongue pulling. The latter intense actions, more prominent in familiar pairs, begin after prolonged immobility and unresponsiveness and cease when the partner regains activity. Their consequences, including improved airway opening and clearance and accelerated recovery from unconsciousness, suggest rescue-like efforts. Oxytocin neurons in the hypothalamic paraventricular nucleus respond differentially to the presence of unconscious versus active partners, and their activation, along with oxytocin signaling, is required for the reviving-like actions. This tendency to assist unresponsive members may enhance group cohesion and survival of social species.

When encountering an individual who has lost consciousness, humans often exhibit emergency responses aimed at reviving that person. Although previous studies of nonhuman animals have documented several types of helping-like behaviors toward conspecifics in need or distress (1–4), whether animals naturally exhibit any distinct behaviors when they encounter a seemingly unconscious (immobilized and unresponsive) peer remains poorly understood.

Anecdotal observations across several species in the wild, including nonhuman primates (5–8), dolphins (9–12), and elephants (13–16), have reported intriguing behaviors of animals toward unresponsive conspecifics that have collapsed because of sickness, injury, or death. These animals often remain close to their incapacitated group members, with increased proximity behaviors (5–16). Additionally, they display various behavioral responses, including touching (5–8, 13–16), grooming (5–8), nudging (6, 9–16), and sometimes even more intense physical actions, such as striking (5, 12), toward the collapsed peers. Some of these actions toward incapacitated conspecifics are reminiscent of human emergency responses, especially those involving sensory stimulation. For instance, in

Western traditions, smelling salts have been used as stimulants to help to restore consciousness (17), and in Eastern traditions, acupuncture of the Ren-Zhong point below the nose is commonly practiced (18). Although the previously reported animal behaviors are thought to be a form of help, given only the scattered observations, it remains challenging to understand the precise nature of these reactions or their generality within a species, let alone to examine their neural underpinnings. In this study, we explored behaviors of laboratory mice in response to and directed toward their unresponsive social partners under controlled conditions, which would allow us to investigate the aforementioned questions.

The stereotypic set of behaviors

We designed an experimental assay to investigate how naïve mice would react to unresponsive or unconscious conspecifics. In the test, a subject mouse in its home cage was presented with a familiar social partner (cagemate) rendered unresponsive through anesthesia or an active counterpart as comparison (Fig. 1A). Behaviors were videotaped, and different types of actions by the subject were annotated through a machine learning-based animal action recognition pipeline (Fig. 1, B and C). The total time of the subject interacting with the unresponsive partner was much greater than with the active counterpart (Fig. 1D). On average, the subject devoted 47.4% of the total testing time interacting with the unresponsive partner, in contrast to only 5.8% with the active counterpart (Fig. 1G). Detailed analysis revealed that the subject increased interactive actions toward the orofacial area, top of the head, trunk, limbs, and tail of the unresponsive partner, as compared with

interactions with the active counterpart (Fig. 1, E and F). The extended interactive actions were the most conspicuous toward the orofacial area, increased by about 15-fold in total duration and consuming on average 31.8% of the total testing time (Fig. 1G).

With the *k*-means clustering analysis on the temporal dynamics of the subject's actions toward the partner, we could classify these actions into three types (Fig. 1H): type 1 involved sniffing of various body parts; type 2 involved gentle physical contact, such as grooming of various body parts; and type 3 involved more forceful physical contact, mostly centered on the eye and mouth areas. As shown by the ethogram of behavioral epochs for a representative subject mouse (Fig. 1I) and the time-dependent plot of probabilities of different types of actions (Fig. 1J), as well as their cumulative durations (Fig. 1K), sniffing and grooming behaviors appeared almost immediately after the introduction of the unresponsive partner, whereas mouth and eye interactions (hereafter, “mouth/eye”) arose with a delay and gradually intensified. Quantification for all the examined pairs showed that mouth/eye interactions appeared later than sniffing and grooming behaviors (fig. S1A). Compared with sniffing, the manifestations of grooming behavior and mouth/eye interaction were more persistent toward the end of the observation window (fig. S1B). In addition, there were more bouts of grooming and mouth/eye interaction than sniffing (fig. S1, C and D), and each bout of mouth/eye interaction lasted longer than sniffing and grooming (fig. S1E). As such, the total duration of mouth/eye interaction was longer than sniffing and grooming (fig. S1F). By contrast, when interacting with an active partner, the subject only exhibited sniffing behaviors that were seen intermittently throughout the test duration (Fig. 1L), whereas grooming and mouth/eye interactions were completely absent (Fig. 1, M and N). Nevertheless, the total duration of sniffing was similar to that when interacting with an unresponsive partner (Fig. 1N). For the latter, sniffing accounted for only 5.9% of the total interaction time, whereas grooming and mouth/eye-targeted actions accounted for 37.8 and 56.3%, respectively (Fig. 1O). Therefore, in comparison to their interactions with active partners, subject mice substantially extended their interaction time with unresponsive partners by engaging in mouth/eye interactions for an extended period of time, a behavior not seen in interactions with an active partner.

Time course of the behavioral actions

For a different cohort, we returned the partner to the home cage immediately after the administration of anesthetics. By doing so, we could monitor the subject's reactions during the partner's gradual shift from a state of wakefulness to unconsciousness (Fig. 2A, top).

¹Center for Neural Circuits and Sensory Processing Disorders, Zilkha Neurogenetic Institute, Keck School of Medicine, University of Southern California, Los Angeles, CA, USA. ²Graduate Program in Biomedical and Biological Sciences, Keck School of Medicine, University of Southern California, Los Angeles, CA, USA. ³Graduate Program in Neuroscience, University of Southern California, Los Angeles, CA, USA. ⁴Department of Physiology and Neuroscience, Keck School of Medicine, University of Southern California, Los Angeles, CA, USA.

*Corresponding author Email: liizhang@usc.edu (L.I.Z); htao@usc.edu (H.W.T.)

†These authors contributed equally to this work.

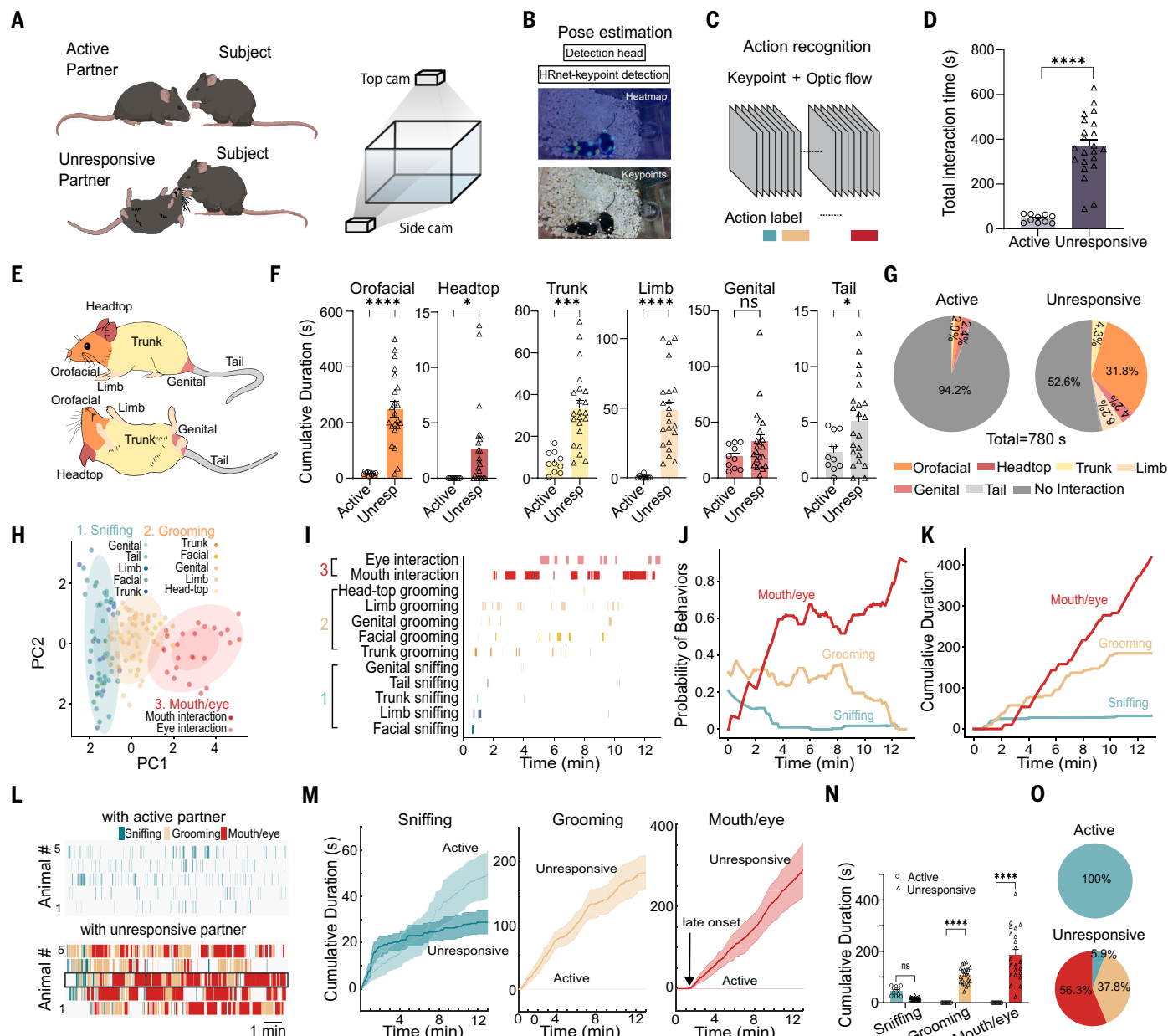


Fig. 1. A stereotypic set of behaviors directed toward an unconscious social partner. (A) Schematic of behavioral setup. (B) Example pose estimation by identifying key points. (C) Schematic of the workflow for action prediction and annotation. (D) Total interaction time with the partner. Unpaired *t* test, ****P* < 0.0001; *n* = 10 and 22 mice for active and unresponsive groups, respectively. (E) Schematic of different body parts. (F) Cumulative durations of actions directed toward different body parts. Columns represent mean \pm SEM. Unpaired *t* test, **P* < 0.05, ****P* < 0.001, *****P* < 0.0001; ns, not significant; *n* = 10 and 22 mice in active and unresponsive groups, respectively. (G) Proportions of total testing time devoted to actions directed toward different body parts. (H) Clustering of different types of actions (labeled by different colors: blue, sniffing; beige, grooming; red, mouth/eye interaction). PC, principal component. (I) Ethogram of different actions for an example subject mouse.

(J and K) Probabilities (J) and cumulative durations (K) of different types of actions over time for the same animal. (L) Ethograms for five example subject mice in active (top) and unresponsive (bottom) groups. (M) Population average of cumulative duration for different types of actions. Note that grooming and mouth/eye-targeted actions were absent in the active group. Shade represents SEM. *n* = 5 animals in each group. (N) Total durations of sniffing, grooming, and mouth/eye interaction toward active (circle) or unresponsive (triangle) partners. Columns represent mean \pm SEM. Two-way ANOVA with Tukey's multiple comparisons test, ****P* < 0.0001; *n* = 10 and 22 animals in active and unresponsive groups, respectively. (O) Proportions of total interaction time devoted to different types of actions in active (top) and unresponsive (bottom) groups (blue, sniffing; beige, grooming; red, mouth/eye interactions). For statistical details, see table S1.

We observed sniffing behaviors immediately after the partner was returned (Fig. 2A, blue, and Fig. 2B). As the partner collapsed and en-

tered a state of complete immobilization (representing an unconscious state), subject mice reduced sniffing and promptly intensified groom-

ing (Fig. 2A, beige, and Fig. 2C). After a period of immobilization of the partner (\sim 100 s), the subject began to direct its actions toward the

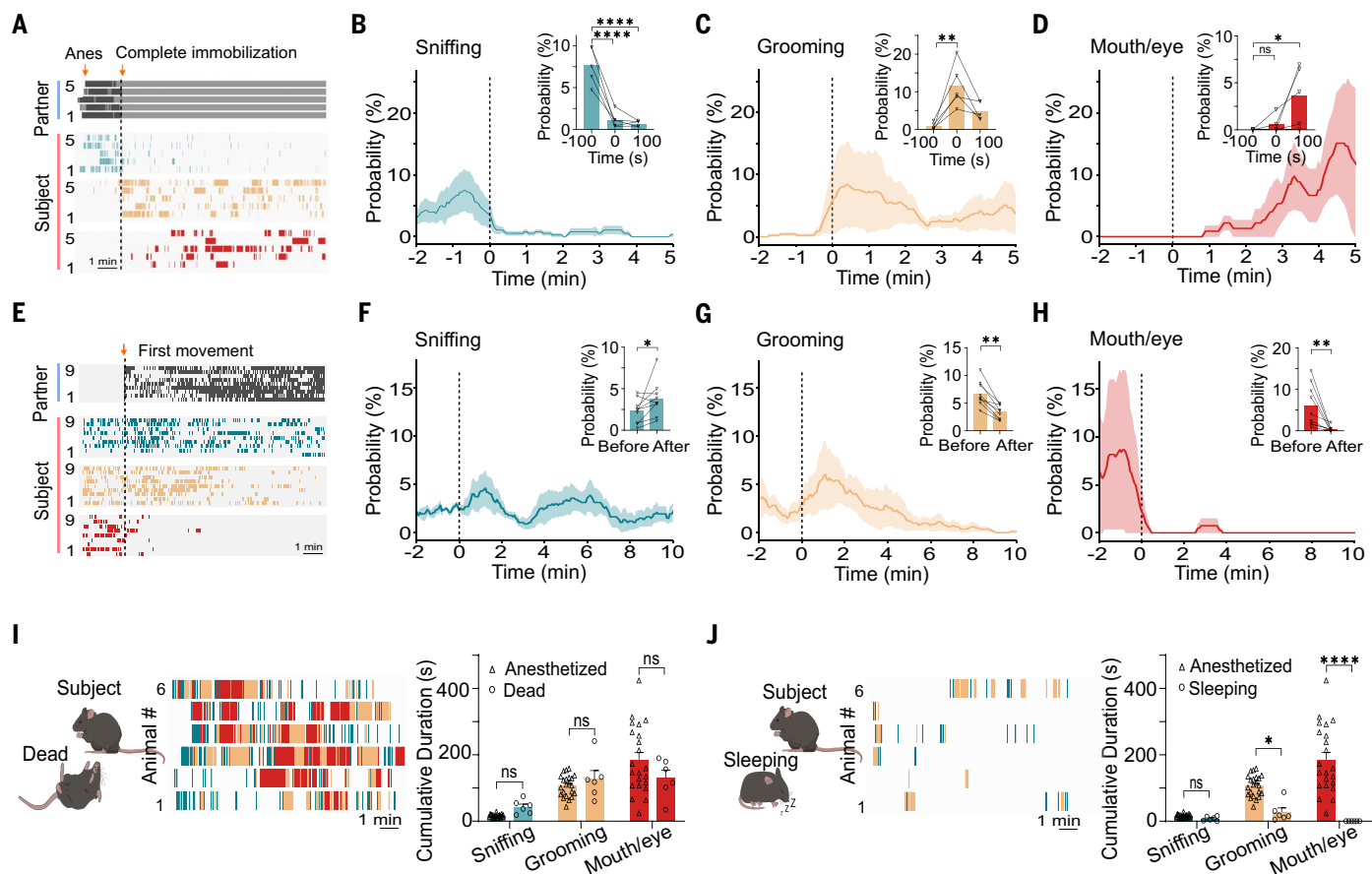


Fig. 2. Behavioral time course and reactions to other states of partners. (A) (Top row) Epochs of active (black) and immobilized (gray) states in the partners aligned with the timing of complete immobilization (marked by the vertical dashed line). (Bottom three rows) Epochs of annotated actions (blue, sniffing; beige, grooming; red, mouth/eye interactions) in the subjects. (B to D) Mean probability of sniffing (B), grooming (C), and mouth/eye interactions (D) aligned with the timing of complete immobility (time point 0). (Insets) Average probability of sniffing, grooming, and mouth/eye interactions within different time windows. One-way repeated measures (RM) ANOVA with Tukey's multiple comparisons test, * $P < 0.05$, ** $P < 0.01$, *** $P < 0.0001$, $n = 5$ animals in each group. (E) (Top row) Epochs of active (black) and immobilized (gray) states in the partners aligned with the timing of the partners' first movement (marked by the vertical dashed line). (Bottom three rows) Epochs of

annotated actions (blue, sniffing; beige, grooming; red, mouth/eye interactions) from the subjects. (F to H) Mean probability of sniffing (F), grooming (G), and mouth/eye interactions (H) aligned with the timing of the partners' first movement (time point 0). (Insets) Average probability of sniffing, grooming, and mouth/eye interactions before versus after the partners' first movement. Wilcoxon test, * $P < 0.05$, ** $P < 0.01$, $n = 9$ animals in each group. (I) Schematic (left) and ethogram (middle) of subject mice's responses to a dead familiar partner, and quantifications of total duration of sniffing, grooming, and mouth/eye interaction toward anesthetized versus dead partners (right). Two-way ANOVA with Tukey's multiple comparisons test; $n = 6$ and 22 animals in dead and anesthetized groups, respectively. (J) Similar to (I), but for actions toward sleeping partners. Two-way ANOVA with Tukey's multiple comparisons test, * $P = 0.0388$, *** $P < 0.0001$; $n = 6$ and 22 animals in sleeping and anesthetized groups, respectively. For statistical details, see table S1.

mouth and eye regions, and these actions gradually intensified (Fig. 2A, red, and Fig. 2D). This analysis suggests that an immobility and unresponsiveness state of the partner promptly triggers grooming behavior and that mouth/eye interactions arise after the subject has witnessed a sustained period of immobility and unresponsiveness.

Next, we investigated how the subject's reactions would change with the partner regaining activity. Isoflurane anesthesia was used to allow a fast recovery so that the subject would experience a sequential transition of the partner's state from unresponsiveness to wakefulness (Fig. 2E). As soon as the partner exhibited the first movement, mouth/eye-targeted actions

by the subject greatly diminished and eventually ceased entirely once the partner became fully awake (Fig. 2H and fig. S2), whereas sniffing increased slightly and grooming declined with a much slower decay after an initial increase (Fig. 2, F and G). Together, our results indicate that the mouth/eye-targeted actions are initiated when the subject is exposed to a prolonged unresponsive state of the partner but are rapidly suppressed once the partner exhibits regained activity and responsiveness. This suggests a correlation between the behavioral manifestation of the subject and the unresponsive state of its social partner.

We sought to determine whether the observed behaviors could be reactions to an unresponsive

state of the partner in general by testing the subject's actions toward a freshly deceased cage mate euthanized by CO₂. Notably, behaviors similar to those toward an anesthetized partner were observed (Fig. 2I and fig. S3). We also analyzed the interaction with a sleeping partner; in this case, the subject exhibited grooming, although to a lesser degree, but never the mouth/eye interactions (Fig. 2J). It is worth noting that while the sleeping partner remained overall inert, it normally responded to the subject's actions with visible movements. Our results are in line with a parallel study showing increased social interactions targeting the head area of a sedated partner compared with an active one (19). Together, these findings suggest that mice are

innately able to differentiate between unresponsive and responsive states of their partners and react to these states differently.

Intense physical interactions and reviving-like effects

Whereas social behaviors of sniffing and allo-grooming have been reported frequently for rodents (2, 3, 20–22), the actions specifically targeting mouth and eye areas seemed peculiar, prompting us to take a closer look by using a high-resolution, high-speed camera providing a side view of the head region. We were then able to distinguish detailed actions such as mouth biting, tongue biting, tongue pulling, and eye licking. Among them, actions directed toward the mouth or tongue were observed in 100% of the animals examined in this experiment (Fig. 3A) and consumed the greatest amount of interaction time (Fig. 3B). After the subject's actions focused on the mouth area, the tongue of the unresponsive partner was pulled out within the test window (Fig. 3C, left four photos, and movie S1) in more than 50% of the cases (Fig. 3C, right). By contrast, in none of the unresponsive mice being alone ("without subject") was the tongue ever observed to spontaneously protrude from the mouth within the test duration (Fig. 3C, right). The tongue pulling action is reminiscent of the medical practice of positioning an unconscious patient's tongue sideways during surgical procedures to prevent potential blockage of the airway (23–26). For unconscious individuals, maintaining an open airway is essential in first aid procedures (27), as muscle relaxation, including that of the tongue, can lead to airway obstruction. Mice with their tongue pulled out had enlarged airways in comparison to those whose tongue remained in their mouth (Fig. 3D), suggesting that a consequence of tongue pulling actions might be to help maintain an open airway in the partner. Accidentally, we discovered that the mouth/tongue-centered behaviors resulted in the removal of a foreign body from the oral cavity of the partner. We then tracked an object artificially placed in the mouth of the unresponsive partner. As shown by a representative pair of mice (Fig. 3E), after the subject started actions that could be described as mouth/tongue biting, the foreign object was removed from the partner's mouth, after which the subject investigated the object for a short period and then resumed the mouth/tongue biting actions (Fig. 3F). Tongue pulling behavior also manifested later on (Fig. 3F). In 80% of cases, the foreign object was successfully removed by the subject's intervention within the test duration (Fig. 3G, left). By contrast, the foreign object was never spontaneously expelled from the partner's mouth in the absence of a subject mouse (Fig. 3G, left). When the foreign object was partially inserted into the anus or genitals, it was ignored and left un-

removed by the subject mouse (Fig. 3G, right). These experiments suggest that the removal of the foreign body might be related to its oral location, with a consequence of further helping with airway clearance when suspected oral obstructions are present.

In the meantime, we observed intermittent body twitching responses in the partner, which temporally correlated with the subject's mouth/tongue biting, tongue pulling, and eye-licking actions (Fig. 3H). In five pairs of mice analyzed, 59 out of 115 mouth/tongue-biting bouts and 18 out of 48 tongue-pulling bouts elicited twitching responses in the partners, whereas 11 out of 17 eye-licking bouts resulted in twitching (Fig. 3I). By contrast, none of the grooming bouts was associated with a twitching response in the partner (Fig. 3I). Cross-correlograms showed a stronger temporal correlation between the twitching response in the partner and mouth/eye-targeted actions than sniffing and grooming actions from the subject (Fig. 3J and K). To further understand the relationship between mouth/eye-targeted actions and body responses of the recipient, we used Von Frey filaments to examine the stimulation threshold at various body parts for eliciting a body twitching response in anesthetized animals; the inner mouth exhibited the lowest threshold compared with other body parts (Fig. 3L). In addition, we stimulated different body parts of lightly anesthetized mice with a Von Frey filament and found that when stimulating the inner mouth, mice exhibited a righting reflex, a potential indicator of arousal (28), after the least number of stimuli (Fig. 3M). These findings raise the possibility that the mouth/tongue biting and tongue pulling actions may provide strong sensory stimulation that can help to arouse the unconscious partner. Indeed, receiving the natural actions from subject mice, the unresponsive partners exhibited the first walk earlier than those left alone (Fig. 3N). Together, our results suggest that the subject's actions, especially those targeting the inner mouth and tongue, may have an effect of helping the partner to recover more quickly from unresponsiveness.

Familiarity, sex, and other features

Previous studies have suggested that familiarity and sex may play a role in social behaviors (29–40). To understand the influence of these factors on the behavioral reactions toward unconscious peers, we explored a variety of different sex combinations under both familiar and unfamiliar conditions. These included male to female (M-F), female to male (F-M), male to male (M-M), and female to female (F-F) pairings (Fig. 4, A and B). Overall, we observed a strong influence of familiarity, as grooming and mouth/eye-targeted actions were much weaker in unfamiliar than familiar pairs, whereas sniffing behaviors were not different between these two conditions (Fig. 4, C to G, and fig. S4, A to

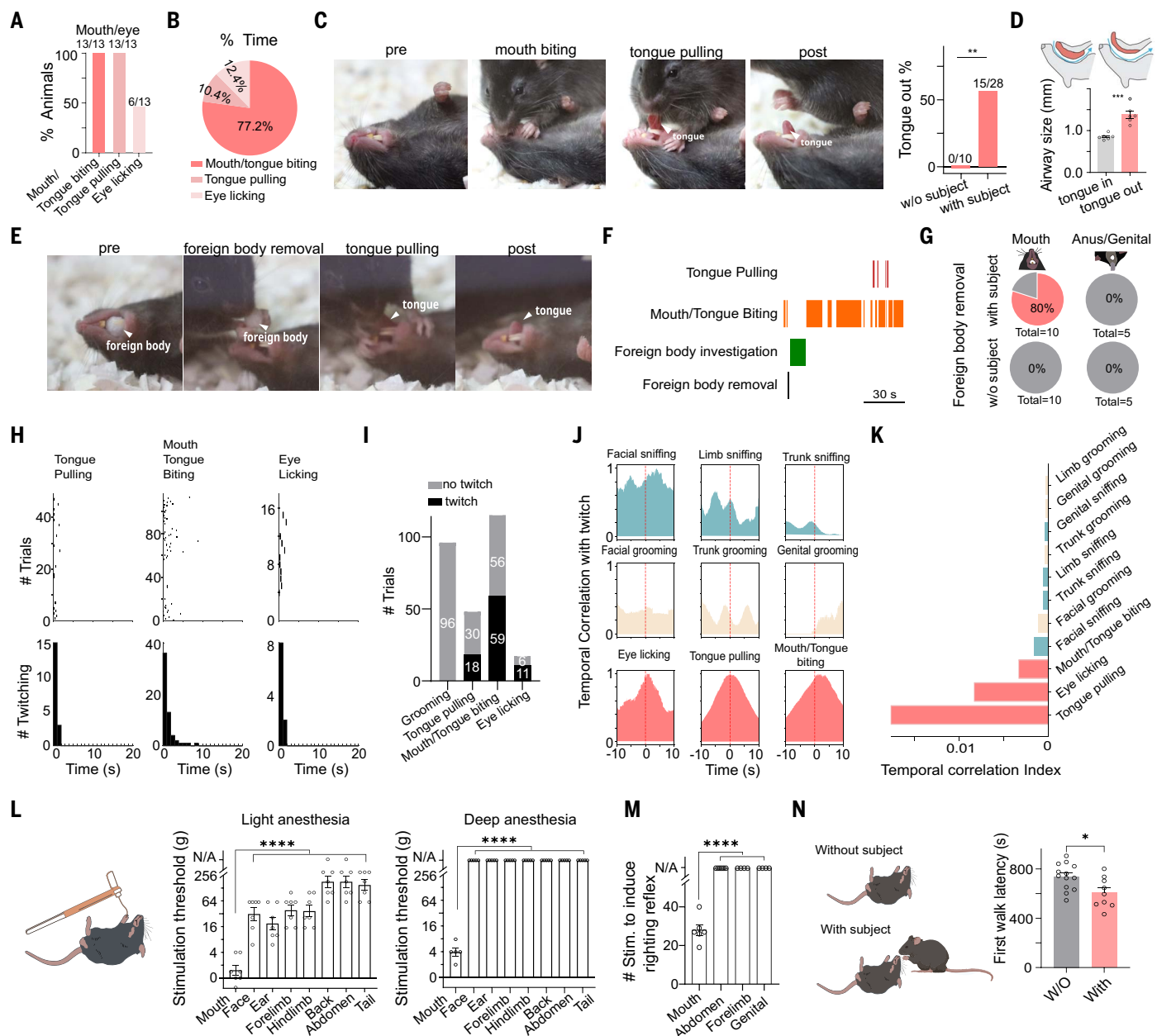
C). Particularly, the mouth/eye-targeted actions were essentially absent in unfamiliar conditions except for the F-F pairing (Fig. 4M). Furthermore, we found that sex plays a rather minor role. In familiar conditions, no differences were observed between different sex-combination groups (Fig. 4, H to J), whereas in unfamiliar conditions, F-F pairing exhibited more prominent allo-grooming and mouth/eye-targeted actions than other pairings (Fig. 4, K to M). Taken together, our results suggest that the behavioral reactions toward unconscious peers as observed in this study are mainly influenced by the familiarity factor and that the intense mouth/eye-targeted actions are prominent between familiar partners of all sex combinations.

To further understand the nature of the behavioral reactions toward unresponsive peers, we investigated whether mice prefer unresponsive social partners over active ones by using a three-chamber social preference test (22, 41, 42). In this test, one side chamber contained an anesthetized animal, and the opposite-side chamber held an active one, with both confined within a small wire cage (Fig. 4N, left). All three animals were females and originated from the same home cage. Measuring the time spent in each chamber revealed a strong preference of the subject to explore the cage containing the unresponsive partner over the active partner (Fig. 4N, right, and Fig. 4O), whereas the subject did not show any preference when both chambers contained an active partner (Fig. 4P). These results argue against the possibility that the subject's attending to an unresponsive peer is driven by pursuit of any potential reciprocal social interaction, as the subject can receive such interaction more immediately by approaching an active peer than an unresponsive one. The preference for an anesthetized peer was not observed when both chambers contained strangers (fig. S4D), which is consistent with the critical impact of familiarity.

Moreover, we asked whether the behavioral reactions to the unresponsive peer would exhibit habituation after repeated exposure to the latter. We performed the same home-cage test repeatedly over 5 consecutive days with the same familiar pair (Fig. 4Q). The time spent interacting remained essentially stable across the 5 days without showing any sign of reduction. Whereas a conspecific in an unresponsive state might be new to the subject when first exposed to it, the apparent absence of habituation suggests that the subject's directing actions toward the peer is not simply driven by novelty seeking or information gathering (43–45).

State-selective activation of PVH oxytocin neurons

To investigate potential neural substrates underlying the behavioral reactions to unresponsive peers, we exposed Trap2::Ai14 mice (46) to either

**Fig. 3. The mouth/eye-targeting actions and their reviving-like effects.**

(A) Percentage of animals exhibiting different mouth/eye interactions. (B) Fraction of time of the total duration of different mouth/eye interactions. (C) Sample images showing the mouth region of an unresponsive partner before and after mouth biting and tongue pulling bouts performed by the subject mouse. White arrowhead marks the tongue. (Right) Percentage incidence of the tongue ending up protruding from the mouth without and with a subject. Chi-square test, ** $P = 0.0029$. (D) Quantification of airway size in mice without and with the tongue pulled out (after fixation). Unpaired t test, *** $P = 0.0002$, $n = 6$ mice in each group. (E) Sample images showing a foreign body in the mouth before and after being removed. (F) Ethogram for an example subject mouse. (G) (Left) Percentage incidence of a foreign object being removed from the mouth (pink) with (top) and without (bottom) a subject. (Right) Percentage incidence of a foreign object being removed from the genital region. (H) Raster plots (top) and event-time histogram (bottom) for the partner's body twitching response

from five pairs of animals. (I) Proportions of action bouts associated with twitching (black) or no twitching (gray). (J) Cross-correlograms between actions and twitching. Bin size, 1 s. Positive values mean that twitch occurred after the initiation of actions. (K) Temporal correlations between different actions and twitching. (L) (Left) Schematic of test of stimulation threshold for inducing twitching responses in an unresponsive animal with Von Frey filaments. (Middle and right) Stimulation threshold at different body parts in lightly and deeply anesthetized animals. One-way ANOVA with Tukey's multiple comparison test, **** $P < 0.0001$, $n = 7$ (left) or 5 (right) animals in each group. (M) Numbers of stimulations at different body parts to induce righting reflex in lightly anesthetized mice with a 4-g Von Frey filament. One-way ANOVA with Tukey's multiple comparison test, **** $P < 0.0001$; $n = 6, 6, 4$, and 4 animals, from left to right. (N) (Left) Schematic of experimental conditions. (Right) Latencies for exhibiting the first walk without (gray) and with (pink) a subject mouse. Unpaired t test, * $P = 0.015$; $n = 13$ and 9 animals, from left to right. For statistical details, see table S1.

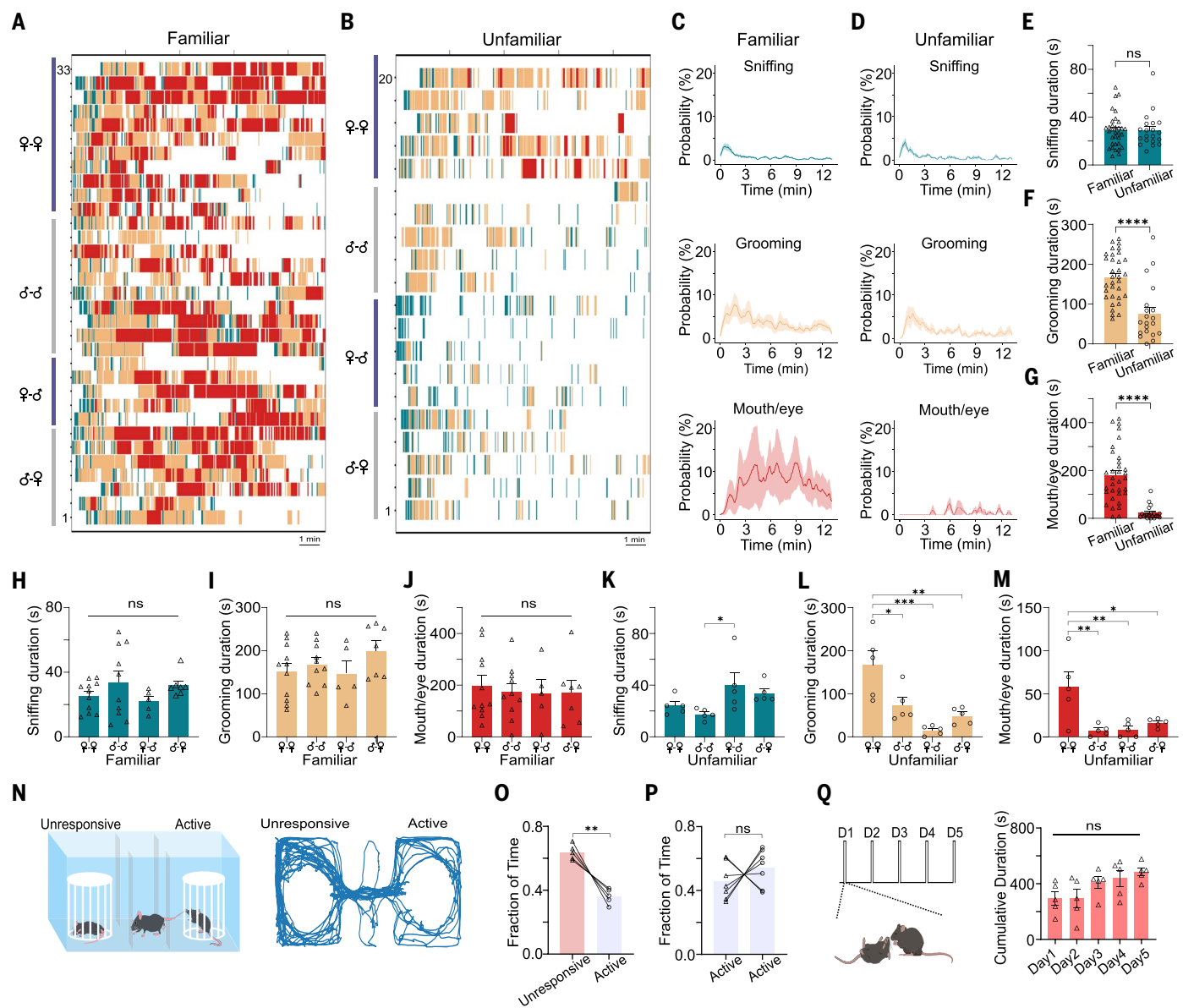


Fig. 4. Factors of familiarity and sex and other features. (A and B) Ethograms for the subject's actions toward an unresponsive conspecific for female-female, male-male, female-male, and male-female pairings in familiar (A) and unfamiliar (B) conditions. Blue, sniffing; beige, grooming; red, mouth/eye interactions. (C and D) Probability of sniffing (top), grooming (middle), and mouth/eye interactions (bottom) in familiar (C) and unfamiliar (D) conditions. Shade represents SEM. (E to G) Total durations of sniffing (E), grooming (F), and mouth/eye interactions (G) toward unresponsive conspecifics in familiar and unfamiliar conditions. Unpaired *t* test, ****P* < 0.0001; *n* = 33 and 20 animals in familiar and unfamiliar groups, respectively. (H to J) Total durations of sniffing (H), grooming (I), and mouth/eye interactions (J) toward unresponsive conspecifics for female-female, male-male, female-male, and male-female

pairings in familiar conditions. One-way ANOVA; *n* = 11, 10, 5, and 7 animals, from left to right. (K to M) Similar to (H) to (J), but for unfamiliar conditions. One-way ANOVA with Tukey's multiple comparisons test, **P* < 0.05, ***P* < 0.01, ****P* < 0.001, *n* = 5 animals in each group. (N) Schematic of three-chamber social preference test (unresponsive versus active; left) and movement tracking traces (right) for an example subject mouse. (O) Fraction of time spent in the side chamber containing an unresponsive versus active partner. Paired *t* test, ***P* = 0.003, *n* = 5 animals. (P) Fraction of time spent in the left versus right side chamber with both containing an active partner. Paired *t* test, *P* = 0.3665, *n* = 7 animals. (Q) Schematic of repeated exposure test over 5 consecutive days (left) and total duration of interactions in each day (right). One-way ANOVA, *P* = 0.0726, *n* = 5 animals. For statistical details, see table S1.

anesthetized or active cagemates. At 1 hour after exposure, we administered 4-hydroxytamoxifen (4-OHT) to label the activated neurons. After 2 weeks of expression, we examined the medial amygdalar nucleus (MEA) (3, 47, 48), paraventricular nucleus of the hypothalamus (PVH)

(2, 49–51), basolateral amygdalar nucleus (BLA) (52–56), hippocampus (57, 58), and ventromedial hypothalamic nucleus (VMH) (59) owing to their potential associations with sniffing, allogrooming, social interaction, or prosocial behaviors. We found that the number of tdTomato+

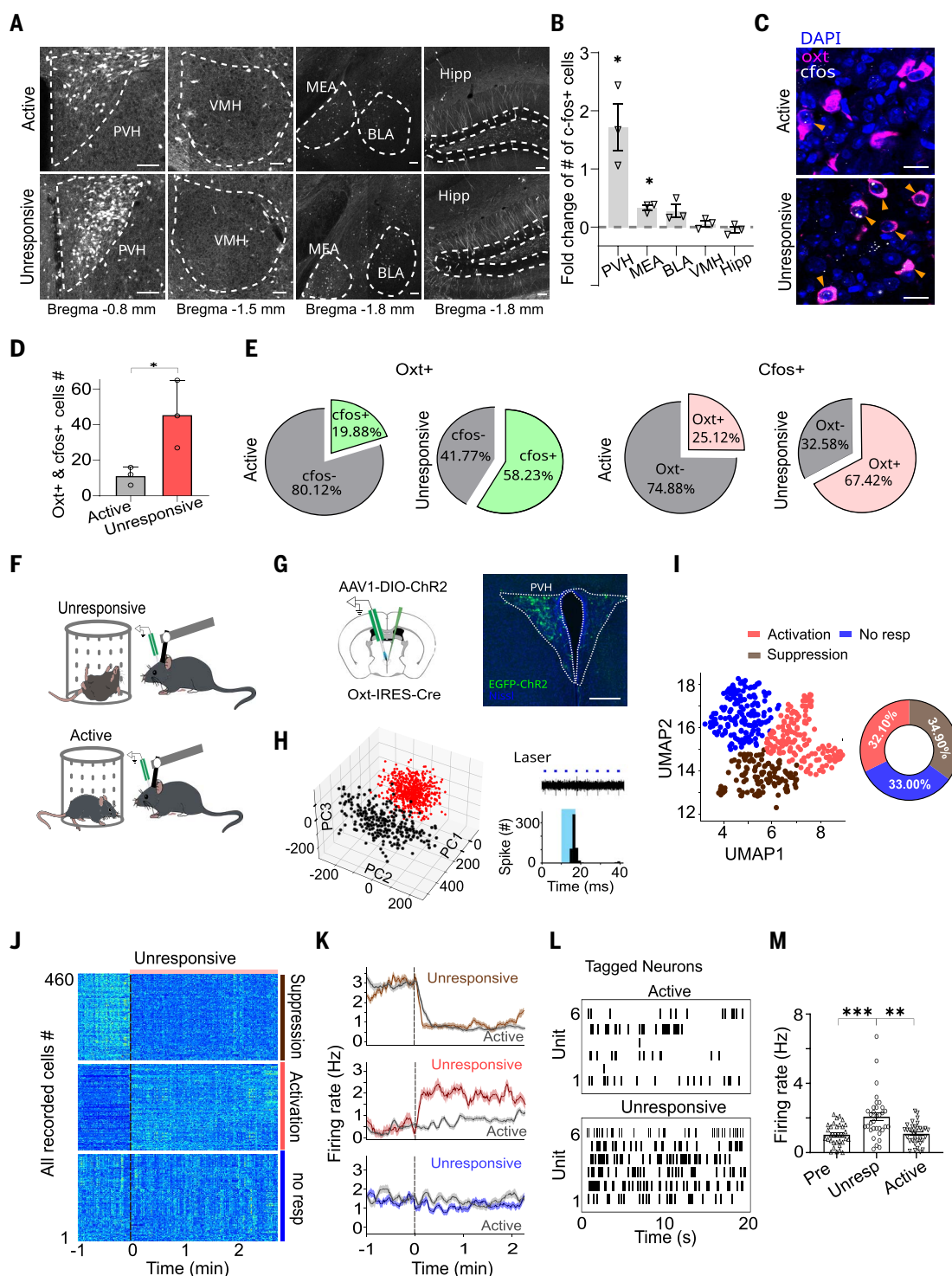
cells, indicative of c-fos expression, was increased in the PVH of mice exposed to unresponsive partners as compared with those exposed to active ones (Fig. 5, A and B), suggesting neuronal activation selective to the exposure to unresponsive partners. As previous studies have implicated

Fig. 5. State-selective activation of PVH oxytocin neurons.

(A) Sample images showing trapped c-fos+ cells in different brain regions of an example subject animal after exposure to an active (top) or unresponsive (bottom) partner. PVH, paraventricular hypothalamic nucleus; VMH, ventromedial hypothalamic nucleus; MEA, medial amygdalar nucleus; BLA, basolateral amygdalar nucleus; Hipp, hippocampus. Scale bars: 100 μ m. **(B)** Fold change in the number of c-fos+ cells in different regions after exposure to unresponsive partners relative to active ones. * $P < 0.05$, one-way ANOVA with Fisher's least significant difference (LSD) multiple comparison test, $n = 3$ animals. Bar represents SEM. **(C)** Representative images of RNA-scope staining of oxytocin (magenta) and c-fos (white) in PVH after exposure to an active (top) or unresponsive (bottom) partner. Arrowheads point to oxytocin neurons that are c-fos+. Scale bars: 20 μ m. **(D)** Number of cells in PVH that are both c-fos+ and oxt+ under two conditions. Unpaired t test, * $P = 0.0390$, $n = 3$ animals in each group.

(E) (Left) Percentage of oxt+ neurons in PVH that are c-fos+ (green). (Right) Percentage of c-fos+ neurons in PVH that are oxt+ (pink). $n = 3$ animals for each condition. **(F)** Schematic of head-fixed in vivo optrode recording in the presence of an unresponsive (top) or active (bottom) partner. **(G)** (Left) Schematic of viral injection and optrode recording in Oxt-Cre mice. (Right) Sample image showing expression of ChR2-EGFP in PVH. Scale bar: 200 μ m.

(H) An example oxytocin unit identified with principal components analysis (left; principal components for all detected spike waveforms from one electrode channel during one recording session) and its spikes time-locked to the laser stimuli (right; upper raw trace and lower peristimulus spike time histogram). **(I and J)** Clustering of all recorded units in PVH and the fraction of cells in each cluster (**I**) and heatmap (**J**) of cells in three clusters aligned to the introduction of an unresponsive partner (vertical dashed line). $N = 460$ units from three animals. **(K)** Population-averaged firing rates for the three clusters before and after the introduction of an unresponsive (color) or an active partner (gray). Shade represents SEM. **(L)** Raster plots of spikes of individual opto-tagged PVH oxytocin neurons in the presence of active (top) or unresponsive (bottom) partners. **(M)** Mean firing rates of oxt+ neurons under different conditions. One-way RM ANOVA with Tukey's multiple comparisons test, ** $P < 0.01$, *** $P < 0.001$, $n = 33$ units from five animals. For statistical details, see table S1.



a role of oxytocin in social (51, 60–68) and prosocial behaviors (2, 4, 69–71), and PVH is one major structure containing oxytocin-releasing neurons (72), we further examined whether PVH oxytocin neurons were activated when exposed to unconscious partners. By conducting RNA-scope staining using probes for *oxytocin* and *c-fos* (Fig. 5C), we found that the number of activated oxytocin neurons was increased in PVH of subject mice exposed to unresponsive partners (Fig. 5D): ~58% of PVH oxytocin neurons were *c-fos*+, and 67% of *c-fos*+ PVH neurons were *oxytocin*+, compared with only 20 and 25%, respectively, in mice exposed to active ones (Fig. 5E).

To directly verify the activation of PVH oxytocin neurons, we expressed channelrhodopsin 2 (ChR2) in these neurons by injecting adeno-associated virus (AAV) encoding Cre-dependent ChR2 in Oxt-Cre mice and performed optrode recording in the awake head-fixed condition (Fig. 5, F to G). An unresponsive or active cagemate confined within a wire cage was presented to the mouse being recorded (Fig. 5F). For all the putative PVH units recorded nonselectively, clustering analysis revealed three groups of neurons: one with an increased firing rate (“activation”), one with a decreased firing rate (“suppression”), and one with no change in the average firing rate (“no response”) when exposed to the unresponsive partner as compared with the pre-exposure condition (Fig. 5, I to J, and fig. S5A). For the “activation” group, the increase in the population-averaged firing rate was larger after exposure to unresponsive partners than to active partners (Fig. 5K, middle), indicating neuronal activation selective to the state of the partner. The oxytocin+ neurons identified in this experiment by their time-locked short-latency spikes to applied light pulses (Fig. 5H) belonged mostly to the “activation” group. For these neurons, a higher mean firing rate was observed when exposed to an unresponsive partner as compared with an active partner and pre-exposure condition (Fig. 5, L and M, and fig. S5B). These data suggest that as the subject detects the unresponsive state of the partner, the activity of oxytocin neurons is increased.

To monitor activity changes from a larger number of oxytocin neurons, we performed microendoscopic (Miniscope) recording of Ca^{2+} signals in freely moving conditions by expressing Cre-dependent GCaMP6s in PVH of Oxt-Cre mice (Fig. 6, A and B). Clustering analysis (Fig. 6C) revealed that a large subset of oxytocin neurons exhibited increased activation during the exposure to unresponsive partners compared with active partners (“unresp”) (fig. S5C). Overall, 51.24% of the imaged neurons showed such selective activation, whereas 10.95% of them showed nonselective activation in both unresponsive- and active-partner conditions (“Both”). As such, the PVH oxytocin neurons

were overall more strongly activated after exposure to unresponsive partners than to active partners (Fig. 6D), consistent with the electrophysiological data. Linear classifiers constructed using the population Ca^{2+} activity of PVH oxytocin neurons could decode unresponsive versus active states of partners with high accuracies (Fig. 6E), suggesting that population activity of oxytocin neurons in each mouse can differentiate between the different states of the partner. Moreover, a more detailed analysis of the selective activation group (Fig. 6C, green) revealed that the increases in activity were correlated well with grooming and mouth/eye-targeted actions (Fig. 6F). This group of neurons could be further classified into three clusters (Fig. 6G), with the largest cluster (cluster 1) exhibiting increased activity associated with both grooming and mouth/eye interaction epochs (Fig. 6, H and I). These results raise the possibility that oxytocin neurons may play a role in the behavioral reactions toward unresponsive partners.

The contribution of oxytocin neurons

To test a possible involvement of oxytocin neurons, we optogenetically silenced PVH oxytocin neurons of subject mice during their exposure to unresponsive cagemates by bilaterally injecting AAV encoding Cre-dependent halorhodopsin (eNpHR3.0) into Oxt-Cre mice (Fig. 7A). The optic silencing (fig. S6, A and B) reduced the subject’s interaction time with the unresponsive partner as compared with the light-off condition in both F-F and M-M pairings (Fig. 7, B and C; fig. S6, C to F; and movie S2). This could be attributed to attenuations of allogrooming and mouth/eye-targeted actions; in comparison, sniffing was not affected (Fig. 7D). Conversely, optogenetically activating PVH oxytocin neurons (at 10 Hz) during the exposure to an unresponsive stranger increased the total interaction time (Fig. 7, E to G, and movie S3), which could be attributed to selective increases in allogrooming and mouth/eye-targeted actions (Fig. 7H and fig. S6, G to J).

Oxytocin signaling has been shown to play a role in social behaviors in rodents (2, 51, 73, 74). As oxytocin affects a broad range of brain structures (74), to test the involvement of oxytocin signaling, we administered an oxytocin receptor antagonist (OTA) through an implanted cannula into the lateral ventricle of subject mice before their exposure to an unresponsive familiar partner (Fig. 7I). In comparison to vehicle injection, blocking oxytocin receptors drastically reduced mouth/eye-targeted actions (Fig. 7, J to L); conversely, self-grooming, rearing, and general locomotion were unaffected (fig. S7). Together, our inactivation and activation experiments support the notion that oxytocin neuron activation and oxytocin signaling are necessary for the expression of the intense stimulatory behaviors toward unresponsive

partners and that enhancing oxytocinergic activity can promote such behaviors.

Discussion

We have elucidated a distinct set of unconditioned behaviors consistently manifested in laboratory mice when they are exposed to an unconscious, unresponsive, or even dead familiar conspecific. Mice show a strong tendency to approach, investigate, and physically interact with the unconscious or unresponsive partner, with their actions escalating chronologically from sniffing and allogrooming to intense stimulatory behaviors targeting orofacial areas, such as mouth or tongue biting and tongue pulling, in response to the continued immobility and unresponsiveness of the partner. Whereas actions such as sniffing and allogrooming are reminiscent of those reported in previous studies on prosocial behaviors directed toward conspecifics in distress or pain (2, 48), the more forceful actions, especially those targeting the inner mouth and tongue that are reported here, are apparently distinctive reactions specifically in response to a prolonged unconscious or unresponsive state of the conspecifics with a delayed onset. Consistent with this idea, similar intense actions can be elicited by exposure to a dead partner, whereas they are absent when exposed to a sleeping partner, which normally responds with visible movements when stimulated by the subject’s actions. Our observations are in line with a parallel study on mouse behaviors toward a sedated peer (19). It remains an outstanding question what sensory cues contribute essentially to the subject’s detection of unresponsive states of the partner. Given the sensitivity of the observed behaviors to body movements of the partner, vision and somatosensation likely play a critical role for the detection and perception of other’s unconscious versus responsive states under our experimental conditions, although involvements of other sensory modalities (19) cannot be excluded.

Our results suggest that the actions of mouth/tongue biting and tongue pulling may have rescue-like effects, reminiscent of human first aid efforts in reviving unconscious individuals with physical stimulation and airway maintenance (27). Although it is challenging to determine the motivational needs behind these distinctive “reviving-like” behaviors as revealed in this study, our experiments suggest that the behaviors may not be driven by the pursuit of reciprocal social interaction or by novelty seeking. On the other hand, the consequences of the behaviors, such as improved airway opening or clearance and expedited recovery, are clearly beneficial to the recipient, similar to helping-like behaviors and other prosocial behaviors (1–3, 75). Given that an unresponsive state in rodents increases their risk of predation, an expedited recovery from unconsciousness, assisted by a

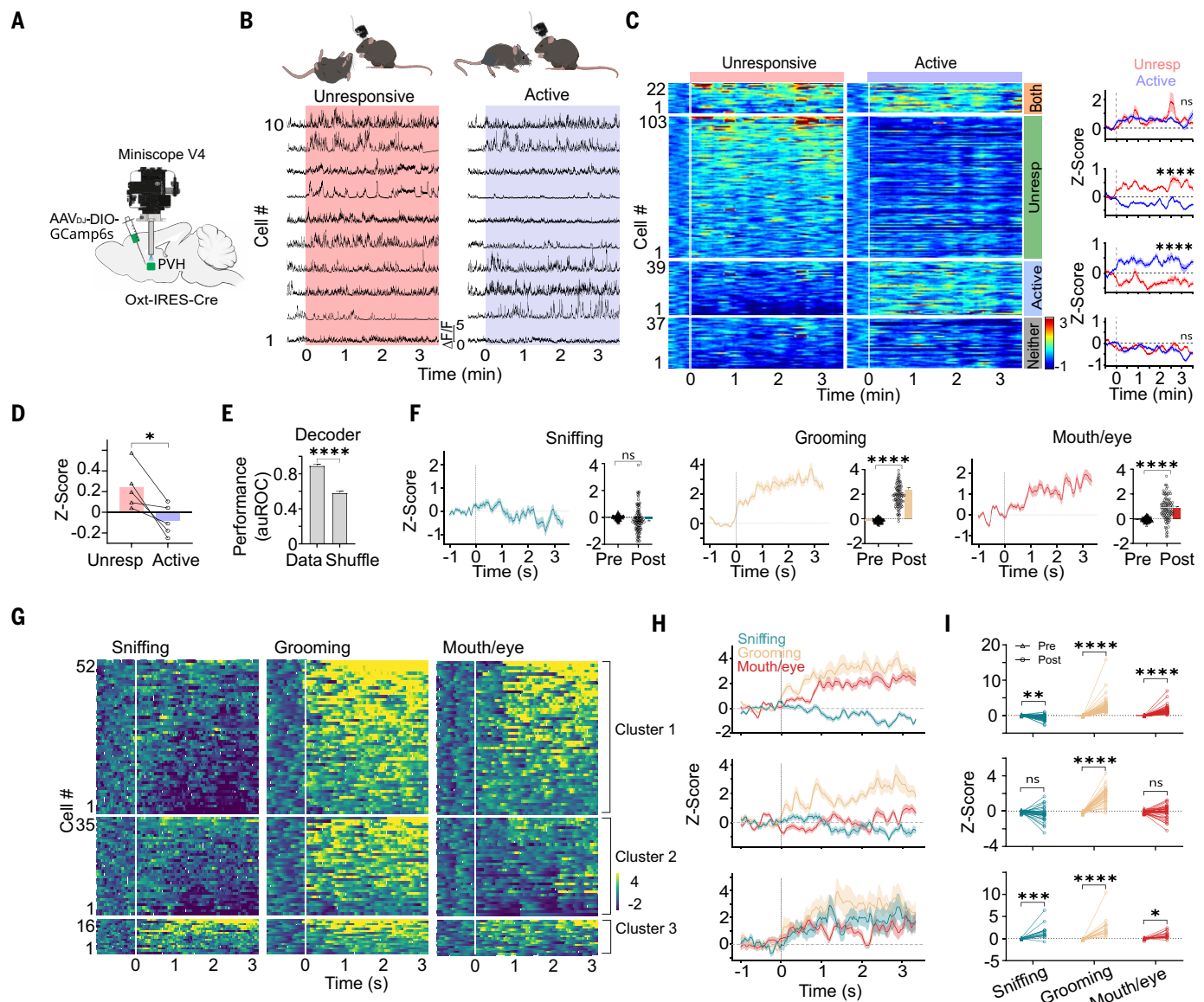


Fig. 6. The unresponsive and active states of the partner are differentially represented by the population activity of PVH oxytocin neurons. (A) Schematic of microendoscope Ca^{2+} imaging. **(B)** $\Delta F/F$ traces of sample PVH oxytocin neurons in response to the introduction (color shade) of an unresponsive (left) or an active (right) partner. **(C)** Heatmaps (left) and population-averaged curves (right) showing the z-score of $\Delta F/F$ dynamics for four clusters of PVH oxytocin neurons in response to the introduction of an unresponsive (red) or an active (blue) partner. Both, responding to both types of partners; Unresp, preferring unresponsive partners; Active, preferring active partners; Neither, no activation to either type. $n = 201$ neurons from five sessions of three animals. Paired t test, unresponsive versus active, $****P < 0.0001$, $n = 22$ neurons for "Both," 103 neurons for "Unresp," 39 neurons for "Active," and 37 neurons for "Neither." **(D)** Mean z-scores of individual sessions for unresponsive versus active partners. Paired t test, $*P < 0.05$, $n = 5$ sessions. **(E)** Performance of decoders trained on the population activity of PVH oxytocin neurons in classifying unresponsive versus

active state of the partner. Unpaired t test, $****P < 0.0001$, $n = 125$ trials in each group. **(F)** Population averaged z-scores of $\Delta F/F$ dynamics (left) and the mean z-score pre- and post-introduction of partners (right) for neurons in the "Unresp" group in response to sniffing (blue), grooming (beige), and mouth/eye interaction (red). Shade represents SEM. Bars and errors represent mean and SEM, respectively. Paired t test, $****P < 0.0001$, $n = 103$ neurons. **(G and H)** Heatmaps (G) and population averaged curves (H) of the z-scored $\Delta F/F$ dynamics for the three clusters in the "Unresp" group, aligned to the onset (time point 0) of sniffing, grooming, or mouth/eye interaction. Shade represents SEM. **(I)** Mean z-scores of $\Delta F/F$ dynamics before versus after the onset of sniffing (blue), grooming (beige), and mouth/eye interaction (red) for the three clusters shown in (H). Two-way RM ANOVA with Fisher's LSD multiple comparisons test, $*P < 0.05$, $**P < 0.01$, $***P < 0.001$, $****P < 0.0001$; $n = 52$, 35, and 16 neurons for clusters 1, 2, and 3, respectively. For statistical details, see table S1.

group member, can greatly enhance the individual's chances of survival.

Also consistent with many prosocial behaviors (29–36, 76, 77), the mouse behavioral ac-

tions toward unresponsive peers in this study exhibit a familiarity bias, particularly for the intense stimulatory actions. The general absence of such actions toward strangers suggests that

the immobility state of a conspecific alone may not be sufficient to drive the behaviors. In addition, these behaviors are only weakly influenced by sex, such that females overall exhibit a

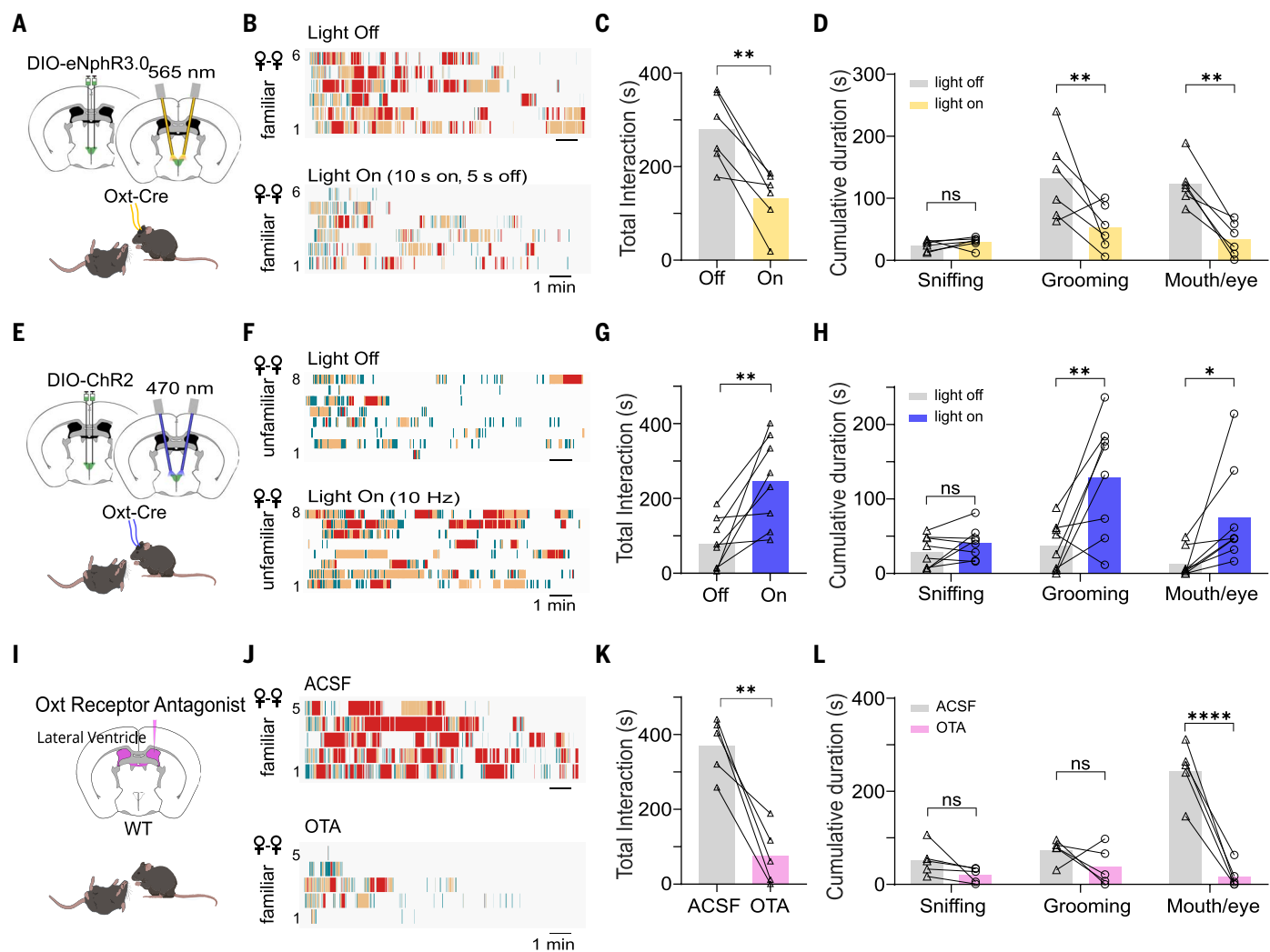


Fig. 7. Manipulating oxytocinergic activity affects the behavioral reactions toward unresponsive peers. (A) Schematic of optogenetic inhibition of PVH oxytocin neurons bilaterally expressing eNpHR3.0. (B) Plots of behavioral epochs of six female subjects presented with unresponsive female partners in light-off (top) and light-on (bottom) conditions. Blue, sniffing; beige, grooming; red, mouth/eye interaction. (C) Cumulative durations of total interactions. Paired *t* test, ***P* < 0.01, *n* = 6 animals. (D) Cumulative durations of sniffing, grooming, and mouth/eye interaction in light-off versus light-on conditions. Two-way RM ANOVA with Bonferroni's multiple comparisons test, ***P* < 0.01, *n* = 6 animals. (E) Schematic of optogenetic activation of PVH oxytocin neurons expressing ChR2. (F) Plots for eight female subjects presented with unresponsive female strangers in light-off (top) and light-on (bottom) conditions.

Blue, sniffing; beige, grooming; red, mouth/eye interaction. (G and H) Similar to (C) and (D), but for optogenetic activation. Paired *t* test in (G) and two-way RM ANOVA with Bonferroni's multiple comparisons test in (H), ***P* < 0.01, **P* < 0.05, *n* = 8 animals. (I) Schematic of injection of an oxytocin receptor antagonist in the lateral ventricle. WT, wild type. (J) Plots of behavioral epochs in five female subjects presented with unresponsive female partners after injection of ACSF vehicle (top) or oxytocin receptor antagonist (bottom). Blue, sniffing; beige, grooming; red, mouth/eye interaction. (K and L) Cumulative durations of total interactions and different types of actions. Paired *t* test in (K) and two-way RM ANOVA with Bonferroni's multiple comparisons test in (L), ***P* < 0.01, ****P* < 0.0001, *n* = 5 animals. For statistical details, see table S1.

slightly stronger tendency than males to interact with unfamiliar conspecifics in unresponsive states. Furthermore, similar to a consolation-like behavior in rodents (2), the oxytocin system plays a pivotal role in regulating the mouse behavioral actions toward unresponsive peers. The unresponsive versus active state of the social partner can be differentiated by the subject on the basis of the population activity of PVH oxytocin neurons of the latter. Activation of the PVH oxytocin neurons and oxytocin signaling are required for the expression of the intense stim-

ulatory behaviors that could be crucial for expediting the recovery of the recipient from the unconscious state. Meanwhile, enhancing oxytocinergic activity can facilitate such behaviors under appropriate contexts. Potential targets of oxytocin that may contribute to these behaviors, such as the prefrontal cortex, amygdala, and nucleus accumbens (74), remain to be examined in the future. Given that the oxytocin system is essentially conserved across vertebrate species (4, 51, 71), combined with previous anecdotal documentations (5–16), our findings in this study

suggest that assisting unresponsive or unconscious group members may be a widely existing behavior among social animals. Such behavior likely plays a role in enhancing the cohesion and survival of the animals as a social group.

Materials and methods

Ethical compliance

All procedures were conducted in accordance with the Guide for the Care and Use of Laboratory Animals, as adopted by the National

Institutes of Health, and with approval of the Institutional Animal Care and Use Committee (IACUC) at the University of Southern California.

Animals

Mice used in this study included C57BL/6J (JAX strain # 000664), Trap2 (JAX strain # 030323), Oxt-IRES-Cre (JAX strain # 024234), and Ai14 (Cre-dependent tdTomato reporter, JAX strain # 007914). All these strains were obtained from Jackson Laboratory. Both male and female adult mice (2 to 3 months old) were used. After weaning, mice were group-housed according to sex, until they underwent surgery or behavioral testing. The living conditions provided to the mice were consistent with a 12-hour light cycle (lights off at 18:00) and unlimited access to food and water.

Viral constructs

AAV vectors used in this study included AAV_{DJ}-EF1a-DIO-GCaMP6s [1.6×10^{13} genome copies (GC/ml, Stanford University Gene Vector and Virus Core, GVVC-AAV-091)], AAV1-pEF1a-DIO-hChR2-eYFP (1.82×10^{13} GC/ml, UPenn vector core), AAV_{DJ}-EF1a-DIO-hChR2-eYFP (3.9×10^{13} GC/ml, Stanford University Gene Vector and Virus Core, GVVC-AAV-038), AAV1-EF1a-DIO-eNpHR3.0-eYFP (2.1×10^{13} GC/ml, Addgene 26966-AAV1), and AAV_{DJ}-EF1a-DIO-NpHR3.0-eYFP (1.6×10^{13} GC/ml, Stanford University Gene Vector and Virus Core, GVVC-AAV-058).

Viral injection

Mice were anesthetized using 1.5 to 5% isoflurane. A minor incision was made on the skin where the craniotomy was planned, followed by removal of the muscles. A craniotomy window was created for each region. AAV encoding different proteins, including GCaMP6s, ChR2, and eNPHR3.0, was introduced per the experiment's purpose and the mouse strain. The virus was delivered (78) using a beveled glass micropipette filled with the viral solution, attached to a microsyringe pump. Pressure injection was used for virus delivery. A small amount of viral solution (50 to 80 nl) was injected at a steady rate (15 to 25 nl/min). After each injection, the pipette was left in place for an additional 5 min before being withdrawn. The skin was then sutured. Before surgery, the pain management drugs buprenorphine and ketoprofen were subcutaneously injected. The mice were allowed a recovery period of at least 1 week before further procedures. After each experiment, the brain was extracted, sectioned, and imaged to confirm viral expression.

Stereotaxic coordinates

The coordinates used for the virus injection and gradient-index (GRIN) lens and fiber implantation in the PVH were as follows. Injection:

anterior-posterior (AP) –0.6 mm, medial-lateral (ML) ±0.2 mm, dorsal-ventral (DV) –4.8 mm. GRIN lens implantation: AP –0.6 mm, ML +0.2 mm, DV –4.7 mm. Fiber implantation: AP –0.6 mm, ML ±1.25 mm, DV –4.5 mm, with a 10° angle. The coordinates used for the cannula implantation in the lateral ventricle were as follows: AP –0.7 mm, ML +1.2 mm, DV –2.5 mm.

Fiber and cannula implantation

For optogenetic manipulations, animals were anesthetized with isoflurane 2 weeks after viral injection, and optic cannulas were bilaterally implanted to target PVH. For pharmacological manipulation, animals were anesthetized with isoflurane, and a drug cannula was stereotactically implanted into the lateral ventricle. The optic cannula or drug cannula was secured with dental cement. The mice were allowed to recover for at least 1 week before the behavior tests. After experiments, the brain was extracted, sectioned, and imaged to confirm the locations of implanted cannulas.

Behavioral tests

Unresponsive, unconscious, and dead animal preparation

The animals were anesthetized using euthasol [50 mg/kg, intraperitoneally (ip)], ketamine (80 mg/kg, ip) and xylazine (8 mg/kg, ip), isoflurane (1 to 5%), or euthanized with CO₂ (100%, 5 min), depending on the purpose of the behavioral tests, as detailed below. The unresponsive state was confirmed on the basis of the loss of voluntary movements and lack of responses to toe pinch, and death was confirmed by the absence of heartbeat and respiration. For animals anesthetized with euthasol, after the test, overdose euthasol (250 mg/kg) was administered for euthanasia.

Test of social behavior toward an unresponsive or unconscious conspecific

Pairs of mice were co-housed for at least 3 days before the behavioral test (79). For each pair, one animal was randomly chosen as the subject, and the other one was assigned as the partner. Animals were allowed to adapt to the handling procedure and the testing environment for two 20-min sessions in two consecutive days before the testing as to minimize stress. The partner was removed from the home cage and anesthetized with euthasol (50 mg/kg, ip), or euthanized with CO₂ (100%, 5 min). After the partner was confirmed to be in an unresponsive state, normally within 10 min of administering anesthesia or euthanasia, it was returned to the home cage. For the control group, the partner was not anesthetized or euthanized but only placed in a separate cage with bedding for ~10 min before being returned to the home cage. The subject's interactions with the unresponsive or active partner in the home cage was videotaped for

13 min. For the test of unfamiliar conditions, the subject and the conspecific were not co-housed before the test.

Mouth foreign object removal test

The procedure was similar to the test described above except that after the partner was in an unresponsive state, a ~4-mm-diameter non-toxic and odorless polyolefin ball was manually placed in its mouth. The partner was then returned to the home cage, and the subject animal's interactions with the unresponsive partner was videotaped for 13 min. For the control test without a subject, the unresponsive animal with a polyolefin ball in the mouth was placed in a new cage alone and was videotaped for 13 min. After the test, the unresponsive animal was euthanized with overdose euthasol (250 mg/kg). For the control experiment, the polyolefin ball was gently and partially inserted into the anus or genitals and was visible to the subject animal.

Body twitching threshold test

We used Von Frey filaments to measure the threshold for eliciting a body twitching response at different body regions of the anesthetized animals, including inner mouth, face, ear, forelimb, hindlimb, back, abdomen, and tail. The testing order of body regions was randomized. For each region, we started with the 0.6-g filament, and enough force was applied to the filament so that it bends slightly and remains in contact for 2 s. If no twitching response was observed, the next higher-level filament would be applied; and if twitching response was observed, the next lower-level filament was used. The lowest force that could induce a twitching response was determined as the threshold for each region. If no twitching response could be elicited using a 300-g filament, the threshold would be marked as not measurable. The duration of the entire test was controlled to be within 20 min. Mice were anesthetized with euthasol at a low dose (40 mg/kg, ip) to induce a light anesthesia state or a higher dose (50 mg/kg, ip) to induce a deep anesthesia state.

First-walk latency test

To measure the first-walk latency with and without a subject animal, isoflurane was used, which allowed the animal to recover in a short period. The partner was put in the induction chamber of the E-Z anesthesia system, and 5% isoflurane was given for 3.5 min and followed by 2% isoflurane for 20 min. After anesthesia, the partner was placed in the home cage with or without the subject mouse. The time point when the animal exhibited the first voluntary walk was determined as the first walk latency. The "first walk" is defined as the animal being able to lift its body off the ground (standing on all four limbs) and take at least two consecutive and coordinated steps. It was

used as an indicator of the animal's recovery from anesthesia.

Wakefulness-to-unresponsiveness transition test

The procedure was similar to that described in the test of social behavior toward an unresponsive conspecific, except that the partner was immediately put back to the home cage after receiving the injection of the anesthetic. In this experiment, the behavior analysis across different animals was aligned to the timing for complete immobilization of the partner. The “complete immobilization” refers to a state in which an animal does not make any movements without another animal’s investigation.

Unresponsiveness-to-wakefulness transition test

The procedure was similar to that described in the test of social behavior toward an unresponsive conspecific, except that the partner was anesthetized with isoflurane. The partner was put in the induction chamber of the E-Z anesthesia system, and 5% isoflurane was given for 3.5 min and followed by 2% isoflurane for 20 min. In this experiment, the behavior analysis across different animals was aligned to the time point when the partner exhibited the first movement or first walk. The “first movement” refers to the first observable movement of any part of the body, such as head lifting, head turning, or limb movement. This marks the earliest sign of recovery from anesthesia, indicating that the animal begins to regain activity. The “first walk” was described in the above “First-walk latency test” section. The “first movement” occurs earlier than the “first walk.”

Righting reflex test

The mouse was put in the induction chamber of the E-Z anesthesia system, and 5% isoflurane was given for 3.5 min and followed by 2% isoflurane for 10 min, during which the induction chamber was placed on top of a heating pad. The animal was then manually stimulated with a 4-g Von Frey filament at 0.5 to 1 Hz frequency. The number of stimulations until when the animal exhibited righting reflex was counted, after which the test was terminated. If the animal did not exhibit the reflex after completing 60 stimulations, the trial was scored as “not measurable,” and the test was terminated.

Familiarity and sex dependency test

Animals were separated into eight groups, depending on the sex combination and familiar or unfamiliar condition. For the familiar groups, same-sex or different-sex pairs were co-housed for at least 3 days before the behavioral testing. For unfamiliar groups, pairs were not co-housed before the behavioral testing. The behavioral test was performed in the

subject animal’s home cage for both familiar and unfamiliar pairs.

Repeated exposure test

The procedure was similar to that described in the test of social behavior toward an unresponsive conspecific, except that we used ketamine (80 mg/kg, ip) and xylazine (8 mg/kg, ip) to anesthetize the partner. We repeated the test once per day for 5 consecutive days. Every day after the test, the anesthetized animal was placed on a heating pad and monitored until it recovered from anesthesia. It was then put back into the home cage.

Social preference test

We used a three-chamber box for this test (41, 80). For the familiar condition, three animals of the same sex and from the same cage were first put in the three-chamber box. After a 60-min habituation period, two of them were randomly chosen and removed from the box. For the active versus anesthetized group, one of the two removed animals was anesthetized with euthasol (50 mg/kg, ip). After the animal was completely anesthetized, it was returned to the testing box and randomly placed in one of the two wire cages placed on opposite sides of the box. And the removed active animal was returned and placed in the other wire cage. For the active versus active group, after 5 min the two animals were returned to the box and respectively placed in one of the two cages. The animal left in the box was designated as the subject animal. For the unfamiliar condition, the subject animal was first put in the three-chamber box for a 60-min habituation period. After that, one anesthetized animal and one active unfamiliar animal were randomly placed in one of the two wire cages placed on opposite sides of the box. The behavior of the subject animal was recorded for 10 min. The place preference index, calculated as the ratio of time spent in each chamber to the total testing time, was automatically determined using custom-developed scripts as described below.

Behavioral annotation

We first batch processed all the recorded videos and extracted featured frames using *k*-means algorithms on the basis of the image hash similarity. Trained human annotators then annotated animal bounding boxes and key points in an iterative process, alongside annotating the start and end times of specific actions in each video, using BORIS (81) and LabelMe. Around 50,000 annotated frames were used in the training of Faster R-CNN (82) and HRNet (83) in object and keypoints detection, and all video clips were used in training the SlowFast network (84) used for action recognition. To further help differentiate actions with small movements, such as sniffing and grooming, optic flow analysis was used, as snif-

fing did not induce optic flow signal changes in the recipient animal, whereas the grooming behavior did. Additionally, automatic annotations were further validated by experimenters to ensure accuracy. The scripts used are available in the GitHub Repository (https://github.com/LiZhangLaboratory/Mouse_keypoint_detection-main), supporting the reliability and validity of our behavioral annotation process. The definitions of different behaviors are as follows. Sniffing is associated with a rapid twitching of the nose or whisking. Owing to the lack of physical contact with the recipient, sniffing would not cause noticeable movement in the latter. Depending on the targeted body parts, sniffing is categorized into subtypes, such as facial sniffing and genital sniffing. Grooming is defined as licking behaviors toward the recipient (e.g., on fur or skin surface), which would cause movements in the latter that can be detected by the frame-by-frame differentiation. Grooming is categorized into different subtypes on the basis of the targeted body parts, such as facial grooming and trunk grooming. Mouth/eye interaction is defined as when the mouse uses its mouth to bite and pull the recipient’s tongue out of its mouth and licks the recipient’s eye region. Detailed actions include the following. (i) Mouth/tongue biting: The subject bites the recipient’s mouth or tongue, often using its forelimbs to stabilize the head of the recipient while shifting the biting location around the mouth. (ii) Tongue pulling: This occurs during mouth/tongue biting, when the subject clamps the recipient’s tongue with its teeth and attempts to pull it out. The action of clamping and pulling the tongue is defined as tongue pulling. (iii) Eye licking: The subject licks the eye regions of the recipient. First start time, last end time, frequency of bouts, interbout interval, duration per bout, and total duration of each behavior were used for clustering, as shown in Fig. 1H. The data were first normalized and then went through dimensional reduction, and *k*-means clustering was performed on the basis of the principal components.

Optrode recording

PVH oxytocin neurons were opto-tagged by injecting AAV-DIO-ChR2 in PVH of Oxt-Cre mice. Before the experiment, subject animals were prepared for awake, head-fixed recordings (85–87). On the day of recording, either an active or anesthetized animal encased within a wire cage was presented to the subject animal, during which neuronal activity was recorded from PVH of the subject. An optrode (A1x64-Poly2-6mm-23s-160-OA64LP, NeuroNexus Technologies) was then connected with an LED light source (470 nm) through an optic fiber. To identify opto-tagged oxytocin neurons, LED light pulse trains varying in frequency (5-ms pulse duration, 2 to 20 Hz) were applied at the end of

each recording trial. The time-locked spikes were detected on the basis of the peristimulus time histogram (PSTH) in response to LED pulses. Only cells that showed LED-related spikes with *z*-score >10 and the PSTH peak being within a 10-ms time window after the onset of each LED pulse were considered as opto-tagged oxytocin neurons. Multiple penetrations were done in each animal, and for each penetration, the animal was presented with a different set of partners. We used a 64-channel probe and were able to obtain roughly 50 units per penetration. Each animal was exposed to no more than three sets of partners. Spike sorting was performed by using Offline Sorter (Plexon). Spike clusters were classified as single units only if the waveform signal-to-noise ratio exceeded 4 (12 dB) and the interspike intervals exceeded 1.2 ms for >99.5% of the spikes.

For the uniform manifold approximation and projection analysis depicted in Fig. 5I, the entire traces of the *z*-scored firing rates from all recorded cells were used as input data. Initially, principal components analysis (PCA) was performed to reduce the dimensionality of the dataset while retaining the most significant variance components. The PCA-transformed data were then subjected to *k*-means clustering. To determine the optimal number of clusters (*k*), we used an iterative approach by systematically varying *k* and evaluating the clustering results. This iterative process involved comparing the response patterns across different clusters using statistical metrics to assess whether the identified patterns were significantly distinct from one another ($P < 0.05$, one-way RM ANOVA test), thereby ensuring that the clustering was neither underfitting nor overfitting the data. This approach is aimed to achieve biologically meaningful and statistically robust clustering, minimizing the likelihood of over-clustering and maximizing the interpretability of the response patterns. To compare firing rates in Fig. 5M, the “Pre” was calculated on the basis of a 2-min window without the presence of another animal. The “Unresp” and “Active” groups were calculated within a 0- to 2-min window after the exposure to a partner of corresponding state.

Microendoscopic calcium imaging

AAV_{DY}-EF1a-DIO-GCaMP6s was injected into the PVH of Oxt-Cre mice, and the GRIN lens (0.5 mm, CLES050GFT100, GoFoton) was implanted 100 μ m above the injection site. We used UCLA Miniscope (V4, open ephys) to image the calcium dynamics of the oxytocin neurons during the subject’s free interactions with the unresponsive or active partner. Subject animals were allowed to interact with partners for ~5 min. Before the imaging session, animals underwent a minimum of two habituation sessions lasting 10 min each in two consecutive days, where they became accustomed to han-

dling and microendoscope attachment in their home cage. During the imaging session, the calcium signal video (20 Hz) and the behavior videos (30 Hz) were recorded simultaneously by the Miniscope and the video camera with the Miniscope-DAQ-QT-Software (<https://github.com/Aharoni-Lab/Miniscope-DAQ-QT-Software>). Cellular calcium signals were extracted with MIN1PIPE (88), a fully automatic MATLAB-based toolbox, including data enhancement, movement correction, and signal extraction (<https://github.com/JinghaoLu/MIN1PIPE>). During MIN1PIPE processing, we visually inspected the isolated region of interest and the associated calcium traces to verify neuronal identity and to remove false-positive regions of interest from the analysis.

The functional types of neuronal population were defined by clustering analysis of the calcium signal. The smoothed *z*-scored $\Delta F/F$ time series, with a moving average window of 300 frames, from all recorded cells were used as input data. PCA analysis was performed to reduce the dimensionality of the dataset while retaining the variance components. The PCA-transformed data were then subjected to *k*-means clustering. To determine the optimal number of clusters (*k*), we used an iterative approach by systematically varying *k* and evaluating the clustering results. This iterative process involved comparing the response patterns across different clusters using statistical metrics to assess whether the identified patterns were significantly distinct from one another. To determine the characteristics of a cluster, paired *t* test was performed between the means before and after the introduction of an unresponsive or an active partner for all neurons in that cluster. The neuronal population exhibiting increased activity in the presence of both unresponsive and active partners was annotated as preferring “Both,” the one exhibiting increased activity only in the presence of anesthetized or active partners was annotated as preferring “Unresponsive” or “Active,” respectively, and one without showing increased activity was annotated as preferring “Neither.”

The binary decoder for distinguishing the states of partners on the basis of the population calcium activity for any given trial was constructed by using the generalized linear regression model (GLM). The performance of the decoder was evaluated by the area under the curve (AUC) of the receiver operating characteristic (ROC) curve when making predictions on the set-aside (holdout) test data. Calcium activity traces within the behavior window from each neuron were standardized with *z*-score normalization and averaged, and then processed with the partial least squares (PLS) regression using the states of partners as response variables. The resulting first two or three PLS components that explained at least 70% of the total variance were retained. Between 20 and

40% of the trials were set aside as the test data, while the remaining trials were used to train a GLM decoder assuming a binomial distribution. Finally, the AUC was calculated on the basis of the predictions from the set-aside test data. The shuffle decoders, representing the chance performance, were also constructed using the same procedure as above but with trial labels randomly permuted and the process repeated 100 times to acquire an average performance.

Pharmacological manipulation

Before behavioral testing, animals underwent a minimum of two 20-min habituation sessions in two consecutive days to minimize stress caused by the experimental handling and drug injection procedures. Before testing, 1 μ l of artificial cerebrospinal fluid (ACSF) saline or the oxytocin receptor antagonist OTA (peptidergic ornithine vasotocin analog, 2.5 ng/ μ l, Bachem) was infused into the lateral ventricle through the implanted cannula. After drug infusion, the subject animal was placed back to the home cage, and the test of social behavior toward an unresponsive conspecific started 30 min later. Behavioral testing was performed on different days for OTA and ACSF.

Optogenetic stimulation

Before behavioral testing, animals underwent a minimum of two habituation sessions lasting 10 min each, where they became accustomed to handling and patch cable tethering in their home cage. Optogenetic manipulations were conducted using an LED light source (470 or 565 nm) which delivered ~5 mW of light through an optic cable, throughout the whole 13-min testing window. For photoactivation with ChR2, 470 nm light was pulsed at 10 Hz with a pulse duration of 10 ms. Photoinhibition used a 565 nm light delivered in a pattern of 10 s on and 5 s off to minimize the desensitization of the opsin and rebound responses. Throughout these procedures, animals were able to move freely within home cages. Customized Python code and Arduino microcontrollers were used to control light delivery for each behavioral assay.

Slice recording

To test the efficacy of halorhodopsin, brain slices were prepared, and whole-cell current-clamp recordings were made from neurons expressing NpHR3.0. Three weeks after injections, animals were decapitated after urethane anesthesia, and the brain was rapidly removed and immersed in an ice-cold dissection buffer (composition, 60 mM NaCl, 3 mM KCl, 1.25 mM NaH₂PO₄, 25 mM NaHCO₃, 115 mM sucrose, 10 mM glucose, 7 mM MgCl₂, 0.5 mM CaCl₂, saturated with 95% O₂ and 5% CO₂; pH 7.4). Coronal slices at a thickness of 350 μ m were sectioned with a vibrating microtome (Leica, VT1000s) and recovered for 30 min in a submersion chamber filled with warmed (35°C) ACSF (composition,

119 mM NaCl, 26.2 mM NaHCO₃, 11 mM glucose, 2.5 mM KCl, 2 mM CaCl₂, 2 mM MgCl₂, 1.2 mM NaH₂PO₄, 2 mM sodium pyruvate, 0.5 mM VC). PVH oxytocin neurons with NpHR3.0-eYFP-expressing were visualized under a fluorescence microscope (Olympus, BX51 WI). Patch pipettes (resistance of ~4 to 5 megohms) filled with a cesium-based internal solution (composition, 125 mM cesium gluconate, 5 mM TEA-Cl, 2 mM NaCl, 2 mM CsCl, 10 mM HEPES, 10 mM EGTA, 4 mM ATP, 0.3 mM GTP, and 10 mM phosphocreatine, pH 7.25; 290 mosmol) were used for whole-cell recordings. Signals were recorded with an Axopatch 700B amplifier (Molecular Devices) under voltage-clamp mode at a holding voltage of -70 mV for excitatory currents, filtered at 2 kHz and sampled at 10 kHz. Yellow light stimulation was applied to measure hyperpolarization in eNpHR3.0-eYFP-expressing neurons.

C-fos trapping

The Trap2 mouse crossed with Ai14 was used to trap c-fos expression as an indicator of neuronal activation. The procedure (89, 90) was similar to that described in the test of social behavior toward an unresponsive conspecific, except that the partner was anesthetized with ketamine (80 mg/kg, ip) and xylazine (8 mg/kg, ip). One hour after the test, the subject mouse was intraperitoneally injected with 50 mg/kg of 4-OHT. Fourteen days after 4-OHT administration, the subject mouse was sacrificed, and the brain was extracted for imaging.

RNAscope analysis

We used C57BL/6J mice in this experiment. At half an hour after the test of social behavior toward an unresponsive conspecific, the subject animal was anesthetized and then perfused with phosphate-buffered saline (PBS) and a 4% solution of paraformaldehyde (PFA). The brain was subsequently dissected and fixed overnight. After fixation, the brain was dehydrated, and cryosections of 30-μm thickness were collected and mounted on Superfrost Plus slides. For RNAscope staining, we used the RNAscope Multiplex Fluorescent Detection Assay V2 kit (Advanced Cell Diagnostics, 323100), following the manufacturer's recommended protocol. Brain sections were hybridized using a mix of RNAscope probes for *c-fos* and *oxytocin*, all of which were designed and validated by Advanced Cell Diagnostics. The signals from these probes were then amplified and marked with fluorescent dyes. Imaging of the samples was conducted using confocal microscopy. The obtained images were then processed using ImageJ software for further analysis.

Image acquisition

To check the expression of enhanced yellow fluorescent protein (eYFP), green fluorescent protein (GFP), or mCherry or fiber and cannula tracks, the animals were deeply anesthetized

using isoflurane (5%) and transcardially perfused with PBS and PFA (4% in PBS). Coronal brain sections (150 μm) were made with a vibratome (Leica Microsystems) and stained with Nissl reagent (Deep Red, Invitrogen) for 2 hours at room temperature. Each slice was imaged under a confocal microscope (Olympus).

Statistics

Sample sizes were selected on the basis of previous experience from related research or literatures (1, 3, 69). Animals were randomly assigned to control and test groups. For animals with multiple assays, the sequence of assays was randomized. Investigators were not blinded to group allocation or data collection, but the analyses of behavioral data were performed blind to the conditions of experiments, as data obtained under different conditions were pooled together for an automatic batch analysis with computer software. Prism version 8 software (GraphPad) was used for statistical analysis. The Kolmogorov-Smirnov test was used to test for normality. One-way analysis of variance (ANOVA) and two-way ANOVA with post hoc multiple comparisons test were used to test significance between multiple groups of samples. For two-group comparison, significance was determined by unpaired *t* test. Paired *t* tests or Wilcoxon tests were used to compare data from the same animal.

REFERENCES AND NOTES

- I. Ben-Ami Bartal, J. Decety, P. Mason, Empathy and pro-social behavior in rats. *Science* **334**, 1427–1430 (2011). doi: [10.1126/science.1210789](https://doi.org/10.1126/science.1210789); pmid: [22158823](https://pubmed.ncbi.nlm.nih.gov/22158823/)
- J. P. Burkett et al., Oxytocin-dependent consolation behavior in rodents. *Science* **351**, 375–378 (2016). doi: [10.1126/science.aac4785](https://doi.org/10.1126/science.aac4785); pmid: [26798013](https://pubmed.ncbi.nlm.nih.gov/26798013/)
- Y. E. Wu et al., Neural control of affiliative touch in prosocial interaction. *Nature* **599**, 262–267 (2021). doi: [10.1038/s41586-021-03962-w](https://doi.org/10.1038/s41586-021-03962-w); pmid: [34646019](https://pubmed.ncbi.nlm.nih.gov/34646019/)
- A. M. Borie, L. J. Young, R. C. Liu, Sex-specific and social experience-dependent oxytocin–endocannabinoid interactions in the nucleus accumbens: Implications for social behaviour. *Philos. Trans. R. Soc. Lond. Ser. B* **377**, 2020057 (2022). doi: [10.1098/rstb.2021.0057](https://doi.org/10.1098/rstb.2021.0057); pmid: [35858094](https://pubmed.ncbi.nlm.nih.gov/35858094/)
- A. De Marco, R. Cozzolino, B. Thierry, Coping with mortality: Responses of monkeys and great apes to collapsed, inanimate and dead conspecifics. *Ethol. Ecol. Evol.* **34**, 1–50 (2022). doi: [10.1080/03949370.2021.1893826](https://doi.org/10.1080/03949370.2021.1893826)
- M. Shimada, W. Yano, Behavioral responses of wild chimpanzees toward a juvenile that suddenly lost its animacy due to a fall accident. *Sci. Rep.* **13**, 16661 (2023). doi: [10.1038/s41598-023-43229-0](https://doi.org/10.1038/s41598-023-43229-0); pmid: [37794020](https://pubmed.ncbi.nlm.nih.gov/37794020/)
- S. Masi, Reaction to allospousal death and to an unanimated gorilla infant in wild western gorillas: Insights into death recognition and prolonged maternal carrying. *Primates* **61**, 83–92 (2020). doi: [10.1007/s10329-019-00745-w](https://doi.org/10.1007/s10329-019-00745-w); pmid: [31446468](https://pubmed.ncbi.nlm.nih.gov/31446468/)
- B. Yang, J. R. Anderson, B.-G. Li, Tending a dying adult in a wild multi-level primate society. *Curr. Biol.* **26**, R403–R404 (2016). doi: [10.1016/j.cub.2016.03.062](https://doi.org/10.1016/j.cub.2016.03.062); pmid: [27218842](https://pubmed.ncbi.nlm.nih.gov/27218842/)
- K. J. Park et al., An unusual case of care-giving behavior in wild long-beaked common dolphins (*Delphinus capensis*) in the East Sea. *Mar. Mamm. Sci.* **29**, E508–E514 (2012).
- S. A. Kuczaj 2nd et al., Underwater observations of dolphin reactions to a distressed conspecific. *Learn. Behav.* **43**, 289–300 (2015). doi: [10.3758/s13420-015-0179-9](https://doi.org/10.3758/s13420-015-0179-9); pmid: [25898942](https://pubmed.ncbi.nlm.nih.gov/25898942/)
- G. Bearzi, M. A. L. Reggente, “Epimeletic behavior” in *Encyclopedia of Marine Mammals*, B. Würsig, J. G. M. Thewissen, K. M. Kovacs, Eds. (Elsevier, ed. 3, 2018), pp. 337–338. doi: [10.1016/B978-0-12-804327-1.00121-7](https://doi.org/10.1016/B978-0-12-804327-1.00121-7)
- G. Bearzi et al., Whale and dolphin behavioural responses to dead conspecifics. *Zoology (Jena)* **128**, 1–15 (2018). doi: [10.1016/j.zool.2018.05.003](https://doi.org/10.1016/j.zool.2018.05.003); pmid: [29801996](https://pubmed.ncbi.nlm.nih.gov/29801996/)
- K. Payne, “3. Sources of social complexity in the three elephant species” in *Animal Social Complexity: Intelligence, Culture, and Individualized Societies*, F. B. M. de Waal, P. L. Tyack, Eds. (Harvard Univ. Press, 2003), pp. 57–86. doi: [10.4159/harvard.9780674419131.c5](https://doi.org/10.4159/harvard.9780674419131.c5)
- J. Poole, *Coming of Age with Elephants: A Memoir* (Hyperion, ed. 1, 1996).
- S. Z. Goldenberg, G. Wittemyer, Elephant behavior toward the dead: A review and insights from field observations. *Primates* **61**, 119–128 (2020). doi: [10.1007/s10329-019-00766-5](https://doi.org/10.1007/s10329-019-00766-5); pmid: [31713106](https://pubmed.ncbi.nlm.nih.gov/31713106/)
- I. Douglas-Hamilton, S. Bhalla, G. Wittemyer, F. Vollrath, Behavioural reactions of elephants towards a dying and deceased matriarch. *Appl. Anim. Behav. Sci.* **100**, 87–102 (2006). doi: [10.1016/j.applanim.2006.04.014](https://doi.org/10.1016/j.applanim.2006.04.014)
- P. McCrary, Smelling salts. *Br. J. Sports Med.* **40**, 659–660 (2006). doi: [10.1136/bjsm.2006.029710](https://doi.org/10.1136/bjsm.2006.029710); pmid: [16864561](https://pubmed.ncbi.nlm.nih.gov/16864561/)
- Y. Meng et al., Traditional Chinese medicine in emergency treatment mechanism and application. *Open Access Emerg. Med.* **12**, 111–119 (2020). doi: [10.2147/OAEM.S244110](https://doi.org/10.2147/OAEM.S244110); pmid: [32431555](https://pubmed.ncbi.nlm.nih.gov/32431555/)
- F. Sun, Y. E. Wu, W. Hong, A neural basis for prosocial behavior toward unresponsive individuals. *Science* **387**, eadq2679 (2025). doi: [10.1126/science.adq2679](https://doi.org/10.1126/science.adq2679)
- D. W. Wesson, Sniffing behavior communicates social hierarchy. *Curr. Biol.* **23**, 575–580 (2013). doi: [10.1016/j.cub.2013.02.012](https://doi.org/10.1016/j.cub.2013.02.012); pmid: [23477727](https://pubmed.ncbi.nlm.nih.gov/23477727/)
- J. J. Nadler et al., Automated apparatus for quantitation of social approach behaviors in mice. *Genes Brain Behav.* **3**, 303–314 (2004). doi: [10.1101/j.1601-183X.2004.00071x](https://doi.org/10.1101/j.1601-183X.2004.00071x); pmid: [15344923](https://pubmed.ncbi.nlm.nih.gov/15344923/)
- J. J. Walsh et al., 5-HT release in nucleus accumbens rescues social deficits in mouse autism model. *Nature* **560**, 589–594 (2018). doi: [10.1038/s41586-018-0416-4](https://doi.org/10.1038/s41586-018-0416-4); pmid: [30089910](https://pubmed.ncbi.nlm.nih.gov/30089910/)
- G. B. Drummond, “Keep a clear airway”. *Br. J. Anaesth.* **66**, 153–156 (1991). doi: [10.1093/bja/66.2.153](https://doi.org/10.1093/bja/66.2.153); pmid: [1817613](https://pubmed.ncbi.nlm.nih.gov/1817613/)
- E. C. Behringer, Approaches to managing the upper airway. *Anesthesiol. Clin. North Am.* **20**, 813–832, vi (2002). doi: [10.1016/S0889-8537\(02\)00045-7](https://doi.org/10.1016/S0889-8537(02)00045-7); pmid: [12512264](https://pubmed.ncbi.nlm.nih.gov/12512264/)
- J. Cracknell, “Airway management” in *Zoo Animal and Wildlife Immobilization and Anesthesia*, G. West, D. Heard, N. Caulkett, Eds. (Wiley, ed. 2, 2014), pp. 53–64. doi: [10.1002/978118792919.ch3](https://doi.org/10.1002/978118792919.ch3)
- S. Taylor, Endotracheal intubation of the dog and cat. *Vet. Nurs.* **13**, 188–193 (2022). doi: [10.12968/vn.2022.13.4.188](https://doi.org/10.12968/vn.2022.13.4.188)
- First Aid Manual: The Authorised Manual of St. John Ambulance, St. Andrew’s Ambulance Association, and the British Red Cross* (Dorling Kindersley, ed. 9, 2009).
- A. Z. Wasilczuk, K. L. Maier, M. B. Kelz, The mouse as a model organism for assessing anesthetic sensitivity. *Methods Enzymol.* **602**, 211–228 (2018). doi: [10.1016/bs.mie.2018.01.008](https://doi.org/10.1016/bs.mie.2018.01.008); pmid: [29588030](https://pubmed.ncbi.nlm.nih.gov/29588030/)
- J. T. Lanzetta, B. G. Englis, Expectations of cooperation and competition and their effects on observers’ vicarious emotional responses. *J. Pers. Soc. Psychol.* **56**, 543–554 (1989). doi: [10.1037/0022-3514.56.4.543](https://doi.org/10.1037/0022-3514.56.4.543)
- S. D. Preston, F. B. M. de Waal, Empathy: Its ultimate and proximate bases. *Behav. Brain Sci.* **25**, 1–20 (2002). doi: [10.1017/S0140525X02000018](https://doi.org/10.1017/S0140525X02000018); pmid: [12625087](https://pubmed.ncbi.nlm.nih.gov/12625087/)
- D. J. Langford et al., Social modulation of pain as evidence for empathy in mice. *Science* **312**, 1967–1970 (2006). doi: [10.1126/science.1128322](https://doi.org/10.1126/science.1128322); pmid: [16809545](https://pubmed.ncbi.nlm.nih.gov/16809545/)
- D. J. Langford et al., Social approach to pain in laboratory mice. *Circ. Neurosci.* **5**, 163–170 (2010). doi: [10.1080/17470910903216609](https://doi.org/10.1080/17470910903216609); pmid: [19844845](https://pubmed.ncbi.nlm.nih.gov/19844845/)
- S. Weckkin, J. H. Masserman, W. Terris Jr., Shock to a conspecific as an aversive stimulus. *Psychon. Sci.* **1**, 47–48 (1964). doi: [10.3758/BF03342783](https://doi.org/10.3758/BF03342783)
- D. G. Rand, V. L. Brescoll, J. A. C. Everett, V. Capraro, H. Barcelo, Social heuristics and social roles: Intuition favors altruism for women but not for men. *J. Exp. Psychol. Gen.* **145**, 389–396 (2016). doi: [10.1037/xge0000154](https://doi.org/10.1037/xge0000154); pmid: [26913619](https://pubmed.ncbi.nlm.nih.gov/26913619/)
- S. Baez et al., Men, women...who cares? A population-based study on sex differences and gender roles in empathy and moral cognition. *PLOS ONE* **12**, e0179336 (2017). doi: [10.1371/journal.pone.0179336](https://doi.org/10.1371/journal.pone.0179336); pmid: [28632770](https://pubmed.ncbi.nlm.nih.gov/28632770/)

36. A. Soutschek *et al.*, The dopaminergic reward system underpins gender differences in social preferences. *Nat. Hum. Behav.* **1**, 819–827 (2017). doi: [10.1038/s41562-017-0226-y](https://doi.org/10.1038/s41562-017-0226-y); pmid: [31024122](https://pubmed.ncbi.nlm.nih.gov/28600000/)
37. H. Chiu *et al.*, A circuit logic for sexually shared and dimorphic aggressive behaviors in *Drosophila*. *Cell* **184**, 507–520.e16 (2021). doi: [10.1016/j.cell.2020.11.048](https://doi.org/10.1016/j.cell.2020.11.048); pmid: [33382967](https://pubmed.ncbi.nlm.nih.gov/33382967/)
38. Y. Isogai *et al.*, Multisensory logic of infant-directed aggression by males. *Cell* **175**, 1827–1841.e17 (2018). doi: [10.1016/j.cell.2018.11.032](https://doi.org/10.1016/j.cell.2018.11.032); pmid: [30550786](https://pubmed.ncbi.nlm.nih.gov/30550786/)
39. C. R. Lee, A. Chen, K. M. Tye, The neural circuitry of social homeostasis: Consequences of acute versus chronic social isolation. *Cell* **184**, 1500–1516 (2021). doi: [10.1016/j.cell.2021.02.028](https://doi.org/10.1016/j.cell.2021.02.028); pmid: [33691140](https://pubmed.ncbi.nlm.nih.gov/33691140/)
40. J. E. Lischinsky, D. Lin, Neural mechanisms of aggression across species. *Nat. Neurosci.* **23**, 1317–1328 (2020). doi: [10.1038/s41593-020-00715-2](https://doi.org/10.1038/s41593-020-00715-2); pmid: [33046890](https://pubmed.ncbi.nlm.nih.gov/33046890/)
41. S. S. Moy *et al.*, Sociability and preference for social novelty in five inbred strains: An approach to assess autistic-like behavior in mice. *Genes Brain Behav.* **3**, 287–302 (2004). doi: [10.1111/j.1601-1848.2004.00076.x](https://doi.org/10.1111/j.1601-1848.2004.00076.x); pmid: [15344922](https://pubmed.ncbi.nlm.nih.gov/15344922/)
42. C. Tao *et al.*, The medial preoptic area mediates depressive-like behaviors induced by ovarian hormone withdrawal through distinct GABAergic projections. *Nat. Neurosci.* **26**, 1529–1540 (2023). doi: [10.1038/s41593-023-01397-2](https://doi.org/10.1038/s41593-023-01397-2); pmid: [37524978](https://pubmed.ncbi.nlm.nih.gov/37524978/)
43. J. D. Harris, Habituation response decrement in the intact organism. *Psychol. Bull.* **40**, 385–422 (1943). doi: [10.1037/h0053918](https://doi.org/10.1037/h0053918)
44. R. N. Hughes, Neotic preferences in laboratory rodents: Issues, assessment and substrates. *Neurosci. Biobehav. Rev.* **31**, 441–464 (2007). doi: [10.1016/j.neubiorev.2006.11.004](https://doi.org/10.1016/j.neubiorev.2006.11.004); pmid: [17198729](https://pubmed.ncbi.nlm.nih.gov/17198729/)
45. M. Ahmadlou *et al.*, A cell type-specific cortico-subcortical brain circuit for investigatory and novelty-seeking behavior. *Science* **372**, eabe9681 (2021). doi: [10.1126/science.abe9681](https://doi.org/10.1126/science.abe9681); pmid: [33986154](https://pubmed.ncbi.nlm.nih.gov/33986154/)
46. L. A. DeNardo *et al.*, Temporal evolution of cortical ensembles promoting remote memory retrieval. *Nat. Neurosci.* **22**, 460–469 (2019). doi: [10.1038/s41593-018-0318-7](https://doi.org/10.1038/s41593-018-0318-7); pmid: [30692687](https://pubmed.ncbi.nlm.nih.gov/30692687/)
47. M. N. Lehman, S. S. Winans, J. B. Powers, Medial nucleus of the amygdala mediates chemosensory control of male hamster sexual behavior. *Science* **210**, 557–560 (1980). doi: [10.1126/science.7423209](https://doi.org/10.1126/science.7423209); pmid: [7423209](https://pubmed.ncbi.nlm.nih.gov/7423209/)
48. M. Zhang, Y. E. Wu, M. Jiang, W. Hong, Cortical regulation of helping behaviour towards others in pain. *Nature* **626**, 136–144 (2024). doi: [10.1038/s41586-023-06973-x](https://doi.org/10.1038/s41586-023-06973-x); pmid: [38267578](https://pubmed.ncbi.nlm.nih.gov/38267578/)
49. M. Matsumoto *et al.*, Indispensable role of the oxytocin receptor for allogrooming toward socially distressed cage mates in female mice. *J. Neuroendocrinol.* **33**, e12980 (2021). doi: [10.1111/jne.12980](https://doi.org/10.1111/jne.12980); pmid: [34057769](https://pubmed.ncbi.nlm.nih.gov/34057769/)
50. M. Engelmann, C. T. Wotjak, R. Landgraf, Direct osmotic stimulation of the hypothalamic paraventricular nucleus by microdialysis induces excessive grooming in the rat. *Behav. Brain Res.* **63**, 221–225 (1994). doi: [10.1016/0166-4328\(94\)90094-9](https://doi.org/10.1016/0166-4328(94)90094-9); pmid: [7999305](https://pubmed.ncbi.nlm.nih.gov/7999305/)
51. R. C. Froemke, L. J. Young, Oxytocin, neural plasticity, and social behavior. *Annu. Rev. Neurosci.* **44**, 359–381 (2021). doi: [10.1146/annurev-neuro-102320-102847](https://doi.org/10.1146/annurev-neuro-102320-102847); pmid: [33823654](https://pubmed.ncbi.nlm.nih.gov/33823654/)
52. C. P. Mosher, P. E. Zimmerman, K. M. Gothard, Neurons in the monkey amygdala detect eye contact during naturalistic social interactions. *Curr. Biol.* **24**, 2459–2464 (2014). doi: [10.1016/j.cub.2014.08.063](https://doi.org/10.1016/j.cub.2014.08.063); pmid: [25283782](https://pubmed.ncbi.nlm.nih.gov/25283782/)
53. D. Jeon *et al.*, Observational fear learning involves affective pain system and Ca_{1.2} Ca²⁺ channels in ACC. *Nat. Neurosci.* **13**, 482–488 (2010). doi: [10.1038/nrn2504](https://doi.org/10.1038/nrn2504); pmid: [20190743](https://pubmed.ncbi.nlm.nih.gov/20190743/)
54. E. Knapska *et al.*, Between-subject transfer of emotional information evokes specific pattern of amygdala activation. *Proc. Natl. Acad. Sci. U.S.A.* **103**, 3858–3862 (2006). doi: [10.1073/pnas.0511302103](https://doi.org/10.1073/pnas.0511302103); pmid: [16497832](https://pubmed.ncbi.nlm.nih.gov/16497832/)
55. M. Mikosz, A. Nowak, T. Werka, E. Knapska, Sex differences in social modulation of learning in rats. *Sci. Rep.* **5**, 18114 (2015). doi: [10.1038/srep18114](https://doi.org/10.1038/srep18114); pmid: [26655917](https://pubmed.ncbi.nlm.nih.gov/26655917/)
56. A. Djerdjaj *et al.*, Social affective behaviors among female rats involve the basolateral amygdala and insular cortex. *PLOS ONE* **18**, e0281794 (2023). doi: [10.1371/journal.pone.0281794](https://doi.org/10.1371/journal.pone.0281794); pmid: [37797037](https://pubmed.ncbi.nlm.nih.gov/37797037/)
57. C. H. Vanderwolf, Hippocampal activity, olfaction, and sniffing: An olfactory input to the dentate gyrus. *Brain Res.* **593**, 197–208 (1992). doi: [10.1016/0006-8993\(92\)91308-2](https://doi.org/10.1016/0006-8993(92)91308-2); pmid: [1450928](https://pubmed.ncbi.nlm.nih.gov/1450928/)
58. D. Kleinfeld, M. Deschênes, N. Ulanovsky, Whisking, sniffing, and the hippocampal theta-rhythm: A tale of two oscillators. *PLOS Biol.* **14**, e1002385 (2016). doi: [10.1371/journal.pbio.1002385](https://doi.org/10.1371/journal.pbio.1002385); pmid: [26890361](https://pubmed.ncbi.nlm.nih.gov/26890361/)
59. M. Liu, A. Nair, N. Coria, S. W. Linderman, D. J. Anderson, Encoding of female mating dynamics by a hypothalamic line attractor. *Nature* **634**, 901–909 (2024). doi: [10.1038/s41586-024-07916-w](https://doi.org/10.1038/s41586-024-07916-w); pmid: [39142338](https://pubmed.ncbi.nlm.nih.gov/39142338/)
60. T. R. Insel, T. J. Hullihan, A gender-specific mechanism for pair bonding: Oxytocin and partner preference formation in monogamous voles. *Behav. Neurosci.* **109**, 782–789 (1995). doi: [10.1037/0735-7044.109.4.782](https://doi.org/10.1037/0735-7044.109.4.782); pmid: [7576222](https://pubmed.ncbi.nlm.nih.gov/7576222/)
61. J. R. Williams, T. R. Insel, C. R. Harbaugh, C. S. Carter, Oxytocin administered centrally facilitates formation of a partner preference in female prairie voles (*Microtus ochrogaster*). *J. Neuroendocrinol.* **6**, 247–250 (1994). doi: [10.1111/j.1365-2826.1994.tb00579.x](https://doi.org/10.1111/j.1365-2826.1994.tb00579.x); pmid: [7920590](https://pubmed.ncbi.nlm.nih.gov/7920590/)
62. H. Hörnberg *et al.*, Rescue of oxytocin response and social behaviour in a mouse model of autism. *Nature* **584**, 252–256 (2020). doi: [10.1038/s41586-020-2563-7](https://doi.org/10.1038/s41586-020-2563-7); pmid: [32760004](https://pubmed.ncbi.nlm.nih.gov/32760004/)
63. J. N. Ferguson *et al.*, Social amnesia in mice lacking the oxytocin gene. *Nat. Genet.* **25**, 284–288 (2000). doi: [10.1038/77040](https://doi.org/10.1038/77040); pmid: [10888874](https://pubmed.ncbi.nlm.nih.gov/10888874/)
64. M. M. Cho, A. C. DeVries, J. R. Williams, C. S. Carter, The effects of oxytocin and vasopressin on partner preferences in male and female prairie voles (*Microtus ochrogaster*). *Behav. Neurosci.* **113**, 1071–1079 (1999). doi: [10.1037/0735-7044.113.5.1071](https://doi.org/10.1037/0735-7044.113.5.1071); pmid: [10571489](https://pubmed.ncbi.nlm.nih.gov/10571489/)
65. H. Walum, L. J. Young, The neural mechanisms and circuitry of the pair bond. *Nat. Rev. Neurosci.* **19**, 643–654 (2018). doi: [10.1038/s41583-018-0072-6](https://doi.org/10.1038/s41583-018-0072-6); pmid: [30301953](https://pubmed.ncbi.nlm.nih.gov/30301953/)
66. A. M. Borin *et al.*, Social experience alters oxytocinergic modulation in the nucleus accumbens of female prairie voles. *Curr. Biol.* **32**, 1026–1037.e4 (2022). doi: [10.1016/j.cub.2022.01.014](https://doi.org/10.1016/j.cub.2022.01.014); pmid: [35108521](https://pubmed.ncbi.nlm.nih.gov/35108521/)
67. S. L. Resendez *et al.*, Social stimuli induce activation of oxytocin neurons within the paraventricular nucleus of the hypothalamus to promote social behavior in male mice. *J. Neurosci.* **40**, 2282–2295 (2020). doi: [10.1523/JNEUROSCI.1515-18.2020](https://doi.org/10.1523/JNEUROSCI.1515-18.2020); pmid: [32024781](https://pubmed.ncbi.nlm.nih.gov/32024781/)
68. S. Yao, J. Bergan, A. Lanjuin, C. Dulac, Oxytocin signaling in the medial amygdala is required for sex discrimination of social cues. *eLife* **6**, e13173 (2017). doi: [10.7554/eLife.31373](https://doi.org/10.7554/eLife.31373); pmid: [29231812](https://pubmed.ncbi.nlm.nih.gov/29231812/)
69. I. Carcea *et al.*, Oxytocin neurons enable social transmission of maternal behaviour. *Nature* **596**, 553–557 (2021). doi: [10.1038/s41586-021-03814-7](https://doi.org/10.1038/s41586-021-03814-7); pmid: [34381215](https://pubmed.ncbi.nlm.nih.gov/34381215/)
70. N. Marsh *et al.*, The neuropeptide oxytocin induces a social altruism bias. *J. Neurosci.* **35**, 15696–15701 (2015). doi: [10.1523/JNEUROSCI.3199-15.2015](https://doi.org/10.1523/JNEUROSCI.3199-15.2015); pmid: [26609161](https://pubmed.ncbi.nlm.nih.gov/26609161/)
71. C. Yoshihara, M. Numan, K. O. Kuroda, Oxytocin and parental behaviors. *Curr. Top. Behav. Neurosci.* **35**, 119–153 (2017). doi: [10.1007/7854_2017_11](https://doi.org/10.1007/7854_2017_11); pmid: [28812267](https://pubmed.ncbi.nlm.nih.gov/28812267/)
72. C. H. Rhodes, J. I. Morrell, D. W. Pfaff, Immunohistochemical analysis of magniocellular elements in rat hypothalamus: Distribution and numbers of cells containing neurophysin, oxytocin, and vasopressin. *J. Comp. Neurol.* **198**, 45–64 (1981). doi: [10.1002/cne.901980106](https://doi.org/10.1002/cne.901980106); pmid: [7014660](https://pubmed.ncbi.nlm.nih.gov/7014660/)
73. M. Manning *et al.*, Oxytocin and vasopressin agonists and antagonists as research tools and potential therapeutics. *J. Neuroendocrinol.* **24**, 609–628 (2012). doi: [10.1111/j.1365-2826.2012.02303.x](https://doi.org/10.1111/j.1365-2826.2012.02303.x); pmid: [22375852](https://pubmed.ncbi.nlm.nih.gov/22375852/)
74. V. Grinevich, I. D. Neumann, Brain oxytocin: How puzzle stones from animal studies translate into psychiatry. *Mol. Psychiatry* **26**, 265–279 (2021). doi: [10.1038/s41380-020-0802-9](https://doi.org/10.1038/s41380-020-0802-9); pmid: [32514104](https://pubmed.ncbi.nlm.nih.gov/32514104/)
75. C. Keysers, E. Knapska, M. A. Moita, V. Gazzola, Emotional contagion and prosocial behavior in rodents. *Trends Cogn. Sci.* **26**, 688–706 (2022). doi: [10.1016/j.tics.2022.05.005](https://doi.org/10.1016/j.tics.2022.05.005); pmid: [35667978](https://pubmed.ncbi.nlm.nih.gov/35667978/)
76. R. B. Cialdini, S. L. Brown, B. P. Lewis, C. Luce, S. L. Neuberg, Reinterpreting the empathy-altruism relationship: When one into one equals oneness. *J. Pers. Soc. Psychol.* **73**, 481–494 (1997). doi: [10.1037/0022-3514.73.3.481](https://doi.org/10.1037/0022-3514.73.3.481); pmid: [9294898](https://pubmed.ncbi.nlm.nih.gov/9294898/)
77. J. Sawyer, The altruism scale: A measure of co-operative, individualistic, and competitive interpersonal orientation. *AJS* **71**, 407–416 (1966). doi: [10.1086/224129](https://doi.org/10.1086/224129); pmid: [5951757](https://pubmed.ncbi.nlm.nih.gov/5951757/)
78. B. Zingg, B. Peng, J. Huang, H. W. Tao, L. I. Zhang, Synaptic specificity and application of anterograde transsynaptic AAV for probing neural circuitry. *J. Neurosci.* **40**, 3250–3267 (2020). doi: [10.1523/JNEUROSCI.2158-19.2020](https://doi.org/10.1523/JNEUROSCI.2158-19.2020); pmid: [32198185](https://pubmed.ncbi.nlm.nih.gov/32198185/)
79. A. H. Tuttle *et al.*, Social propinquity in rodents as measured by tube cooccupancy differs between inbred and outbred genotypes. *Proc. Natl. Acad. Sci. U.S.A.* **114**, 5515–5520 (2017). doi: [10.1073/pnas.1703477114](https://doi.org/10.1073/pnas.1703477114); pmid: [28484016](https://pubmed.ncbi.nlm.nih.gov/28484016/)
80. C. Tao *et al.*, Excitation-inhibition imbalance in medial preoptic area circuits underlies chronic stress-induced depression-like states. *Nat. Commun.* **15**, 8575 (2024). doi: [10.1038/s41467-024-52727-2](https://doi.org/10.1038/s41467-024-52727-2); pmid: [39362860](https://pubmed.ncbi.nlm.nih.gov/39362860/)
81. O. Friard, M. Gamba, BORIS: A free, versatile open-source event-logging software for video/audio coding and live observations. *Methods Ecol. Evol.* **7**, 1325–1330 (2016). doi: [10.1111/2041-210X.12584](https://doi.org/10.1111/2041-210X.12584)
82. S. Ren, K. He, R. Girshick, J. Sun, Faster R-CNN: Towards real-time object detection with region proposal networks. [arXiv:1506.01497](https://arxiv.org/abs/1506.01497) [cs.CV] (2016).
83. K. Sun, B. Xiao, D. Liu, J. Wang, Deep high-resolution representation learning for human pose estimation. [arXiv:1902.09212](https://arxiv.org/abs/1902.09212) [cs.CV] (2019).
84. C. Feichtenhofer, H. Fan, J. Malik, K. He, SlowFast networks for video recognition. [arXiv:1812.03982](https://arxiv.org/abs/1812.03982) [cs.CV] (2019).
85. G.-W. Zhang *et al.*, Medial preoptic area antagonistically mediates stress-induced anxiety and parental behavior. *Nat. Neurosci.* **24**, 516–528 (2021). doi: [10.1038/s41583-020-00784-3](https://doi.org/10.1038/s41583-020-00784-3); pmid: [33526942](https://pubmed.ncbi.nlm.nih.gov/33526942/)
86. X. Wang *et al.*, A cross-modality enhancement of defensive flight via parvalbumin neurons in zona incerta. *eLife* **8**, e42728 (2019). doi: [10.7554/eLife.42728](https://doi.org/10.7554/eLife.42728); pmid: [30985276](https://pubmed.ncbi.nlm.nih.gov/30985276/)
87. Z. Li *et al.*, Enhancement and contextual modulation of visuospatial processing by thalamocollateral projections from ventral lateral geniculate nucleus. *Nat. Commun.* **14**, 7278 (2023). doi: [10.1038/s41467-023-43147-9](https://doi.org/10.1038/s41467-023-43147-9); pmid: [37949869](https://pubmed.ncbi.nlm.nih.gov/37949869/)
88. J. Lu *et al.*, MINIPIPE: A Miniscope 1-photon-based calcium imaging signal extraction pipeline. *Cell Rep.* **23**, 3673–3684 (2018). doi: [10.1016/j.celrep.2018.05.062](https://doi.org/10.1016/j.celrep.2018.05.062); pmid: [29925007](https://pubmed.ncbi.nlm.nih.gov/29925007/)
89. Y. J. Kim *et al.*, Dcc mediates functional assembly of peripheral auditory circuits. *Sci. Rep.* **6**, 23799 (2016). doi: [10.1038/srep23799](https://doi.org/10.1038/srep23799); pmid: [27040640](https://pubmed.ncbi.nlm.nih.gov/27040640/)
90. J. Wei *et al.*, A distributed auditory network mediated by pontine central gray underlies ultra-fast awakening in response to alerting sounds. *Curr. Biol.* **34**, 4597–4611.e5 (2024). doi: [10.1016/j.cub.2024.08.020](https://doi.org/10.1016/j.cub.2024.08.020); pmid: [39265569](https://pubmed.ncbi.nlm.nih.gov/39265569/)
91. Dr. Li I. Zhang Laboratory, Reviving-like Prosocial Behavior in Response to Unconscious or Dead Conspecifics in Rodents, version 1, Zenodo (2024); <https://doi.org/10.5281/zenodo.14286282>.

Downloaded from https://www.science.org at Virginia Commonwealth University on August 02, 2025

SUPPLEMENTARY MATERIALSscience.org/doi/10.1126/science.adq2677

Figs. S1 to S7

Table S1

MDAR Reproducibility Checklist

Movies S1 to S3

Submitted 6 May 2024; accepted 7 December 2024

[10.1126/science.adq2677](https://doi.org/10.1126/science.adq2677)